The energy minimization problem for two-level dissipative quantum systems

B. Bonnard, Olivier Cots, D. Sugny, Nataliya Shcherbakova

▶ **To cite this version:**

B. Bonnard, Olivier Cots, D. Sugny, Nataliya Shcherbakova. The energy minimization problem for two-level dissipative quantum systems. Journal of Mathematical Physics, 2010, 51 (9), pp.44. 10.1063/1.3479390 . hal-04177744

HAL Id: hal-04177744
https://hal.science/hal-04177744v1

Submitted on 5 Aug 2023

HAL is a multi-disciplinary open access archive for the deposit and dissemination of scientific research documents, whether they are published or not. The documents may come from teaching and research institutions in France or abroad, or from public or private research centers.

L'archive ouverte pluridisciplinaire **HAL**, est destinée au dépôt et à la diffusion de documents scientifiques de niveau recherche, publiés ou non, émanant des établissements d'enseignement et de recherche français ou étrangers, des laboratoires publics ou privés.

The energy minimization problem for two-level dissipative quantum systems

B. Bonnard,[1,a)] O. Cots,[2] N. Shcherbakova,[1] and D. Sugny[3,b)]
[1]*Institut de Mathématiques de Bourgogne, UMR CNRS 5584, BP 47870, 21078 Dijon, France*
[2]*IRIT, ENSEEIHT, UMR CNRS 5055, 31062 Toulouse, France*
[3]*Laboratoire Interdisciplinaire Carnot de Bourgogne (ICB), UMR 5209 CNRS-Université de Bourgogne, 9 Av. A. Savary, BP 47 870, F-21078 Dijon Cedex, France*

(Received 19 November 2009; accepted 23 July 2010; published online 15 September 2010)

In this article, we study the energy minimization problem of dissipative two-level quantum systems whose dynamics is governed by the Kossakowski–Lindblad equations. In the first part, we classify the extremal curve solutions of the Pontryagin maximum principle. The optimality properties are analyzed using the concept of conjugate points and the Hamilton–Jacobi–Bellman equation. This analysis completed by numerical simulations based on adapted algorithms allows a computation of the optimal control law whose robustness with respect to the initial conditions and dissipative parameters is also detailed. In the final section, an application in nuclear magnetic resonance is presented.
[doi:10.1063/1.3479390]

I. INTRODUCTION

In this article, we consider the *energy minimization problem*: $\min \int_0^T (u_1^2(t)+u_2^2(t))dt$ with fixed transfer time T for steering an initial state q_0 to a final state q_1, where $q=(x,y,z)$ and the dynamics is given by the control system,

$$\dot{x} = -\Gamma x + u_2 z,$$

$$\dot{y} = -\Gamma y - u_1 z,$$

$$\dot{z} = \gamma_- - \gamma_+ z + u_1 y - u_2 x. \tag{1}$$

This system is deduced from *Kossakowski–Lindblad* equations[22,32] describing the dynamics of two-level dissipative quantum systems in the rotating wave approximation.[11] Also up to a proper renormalization, it corresponds to the Bloch equation in nuclear magnetic resonance (NMR) when the detuning term is zero.[31] The set $\Lambda=(\Gamma,\gamma_+,\gamma_-)$ is the set of dissipative parameters satisfying the constraints $2\Gamma \geqslant \gamma_+ \geqslant |\gamma_-|$, the control is the complex function $u=u_1+iu_2$ associated with the physical control, which is an electromagnetic field. The cost corresponds to the energy transfer between the control field and the internal Hamiltonian and is an important physical issue.[4,5] The *Bloch ball* $|q|\leqslant 1$, which is the physical state space of the system, is invariant for the dynamics.

Such a control problem is motivated by two recent experimental research projects. The first one concerns the control of the rotation of a molecule in a gas phase by using laser fields[37] and the second deals with the control of the spin dynamics by a magnetic field in NMR.[31] This second problem is the ideal testbed for the application of optimal control to quantum systems since the dissipative parameters can be identified with a great accuracy and all the computed trajectories can

a)Electronic mail: bernard.bonnard@u-bourgogne.fr.
b)Electronic mail: dominique.sugny@u-bourgogne.fr.

be tracked experimentally.[3,25,26,28,31] For the first problem, the experimental situation is more complex since many levels have to be taken into account, but our derived numerical schemes are promising even in this case.[42]

The use of recent geometric control techniques to analyze quantum control systems is a new challenge in optimal control. In this context, many articles are devoted to the conservative case, e.g., see Refs. 4, 5, 16, 17, and 26. The aim of our research program is to extend the analysis to the dissipation case.[34,38] In a first series of articles,[11,14,15,39] we have considered the time-minimal control problem with a control bound $|u| \leqslant M$. The departing framework for the time-minimum and energy minimization problems is the same. Writing the control system in the form

$$\dot{q} = F_0(q) + \sum_{i=1}^{2} u_1 F_i(q),$$

the *Pontryagin maximum principle*[36] tells us that for the time-minimal control problem, outside a surface Σ: $H_i = 0$, $i = 1, 2$, where H_i denotes the Hamiltonian lift $\langle p, F_i(q) \rangle$ of the vector field F_i, the optimal trajectories are selected among a set of *extremal curves* solutions of the Hamiltonian vector field $\vec{H}$ with the Hamiltonian,

$$H = H_0 + (H_1^2 + H_2^2)^{1/2},$$

while for the energy minimization problem, the corresponding Hamiltonian (in the normal case) is given by

$$H = H_0 + \frac{1}{2}(H_1^2 + H_2^2).$$

Despite similar Hamiltonians, the analysis of this article for the energy minimization problem compared with the one of the time-minimal control problem will show significant different results. Two reasons can be mentioned to explain this discrepancy. The first one is technical: for the time-minimal control problem, the Hamiltonian vector field $\vec{H}$ is not smooth on the surface Σ and this leads to behaviors of extremal curves that are complicated to analyze. For the energy minimization problem, it remains smooth on the whole space and asymptotic behaviors are related to those of smooth Hamiltonian vector fields. In this latter case, the normal extremals are associated with a *mechanical system* with potential V and many qualitative properties can be deduced from the graph of V only.

The two optimal control problems are similar for a specific value of the parameters: if $\gamma_- = 0$ and $\gamma_+ = \Gamma$, both cases amount to analyze a *quasi-Riemannian* problem on the two-sphere of revolution given by the *Grushin metric*: $g = d\phi^2 + \tan^2 \phi d\theta^2$, where ϕ is the angle along a meridian, while θ is the angle of revolution along the z-axis. For such a metric, a complete analysis is contained in Ref. 8 where the extremal curves are of two types: meridian circles and ϕ-periodic orbits winding around the equator. Moreover, the conjugate and cut loci have been explicitly described. The energy minimization problem amounts to generalize this program by a classification of the extremal curves and an optimality analysis. In addition, the robustness properties with respect to the dissipative parameters, which are an important physical issue, will be discussed.

This article is organized in three sections. In the first section, we present a classification of the extremal flow, in both abnormal and normal cases. In the normal case, using spherical coordinates, the Hamiltonian takes the form

$$H = p_\rho(\gamma_- \cos\phi - \rho(\delta \cos^2\phi + \Gamma)) + p_\phi\left(-\frac{\gamma_-}{\rho}\sin\phi + \delta \sin\phi\cos\phi\right) + \frac{1}{2}(p_\phi^2 + p_\theta^2 \cot^2\phi),$$

where $\delta = \gamma_+ - \Gamma$. It can be interpreted as a deformation of the Grushin case that occurs for $\gamma_- = 0$ and $\delta = 0$. Extremal curves can be classified in two classes. When $p_\theta = 0$, this corresponds to curves in meridian planes, which restricts the system to the two-dimensional (2D)-plane (y, z) controlled with a real field only. A complete classification of the extremal curves is given, splitting

the analysis into two parts, the case $\gamma_-=0$ where the system is integrable, while for $\gamma_-\neq 0$, only the asymptotic properties of the extremals are described. In the case $p_\theta\neq 0$, again the analysis splits into two parts. The first one is the integrable case $\gamma_-=0$, where we have two types of extremal curves, that is, *short* periodic curves not crossing the equator and *long* periodic curves crossing the equator, which are deformations of the extremal curves of the Grushin case. In both cases, we give a parametrization of the extremals using *elliptic functions*. In the general situation $\gamma_-\neq 0$, the analysis is less complete but the asymptotic behaviors of the solutions can be described in the framework of Hamiltonian dynamics. In Sec. III, the geometric analysis of the extremal flow is used to deduce the optimality properties of the extremals. The problem is to compute the *first conjugate point* where an extremal ceases to be locally optimal for the C^1-topology on the set of curves and the *cut point* where it ceases to be globally optimal. They will form, respectively, the conjugate and cut loci. We introduce the Hamilton–Jacobi–Bellman equation whose integration gives the *value function* and the *isocost spheres*, which are the level sets of the value function. Since the value function solution of the Hamilton–Jacobi–Bellman equation is constructed with the concept of central field, the classification of extremals leads to the computation of *microlocal solutions* which have to be glued together to deduce the global solution. This problem can be handled by computing the conjugate and cut loci. From the general theory (see Ref. 9), the conjugate points can be computed using the variational equation. One can get geometric estimates of such points in the integrable case $\gamma_-=0$, while in the general situation $\gamma_-\neq 0$, we obtain numerical estimates. The final section is devoted to the algorithms and the numerical simulations based on our geometric discussion to conclude the analysis. Several codes developed in a parallel research project in orbital transfer are used:[9] shooting method, computation of Jacobi fields related to the concept of conjugate points, and a numerical continuation scheme where the homotopy parameter λ is related to the dissipative parameters $\delta=\gamma_+-\Gamma$ and γ_-. As a conclusion, we present an application to nuclear magnetic resonance (NMR), comparing the energy-minimal trajectory to the time-minimal trajectory.

II. GEOMETRIC ANALYSIS OF THE EXTREMAL CURVES

A. Maximum principle

First of all, we recall some standard results concerning the maximum principle needed in our computations (see Ref. 10 for the details). Consider the energy minimization problem: $\min_{u(\cdot)}\int_0^T\Sigma_{i=1}^m u_i^2(t)dt$, where the transfer time T is fixed for a smooth system of the form: $\dot{q}=F_0(q)+\Sigma_{i=1}^m u_iF_i(q)$ on a smooth manifold M and where the set of admissible controls $\mathcal{U}$ is the set of bounded measurable mapping $u:[0,T]\to\mathbb{R}^m$ such that the corresponding trajectory $q(\cdot,u,q_0)$, initiating from q_0 is defined on the whole interval.

According to the maximum principle, the optimal solutions are a subset of a set of *extremal curve* solutions of the equations,

$$\frac{dq}{dt}=\frac{\partial\tilde{H}}{\partial p},\quad \frac{dp}{dt}=-\frac{\partial\tilde{H}}{\partial q}, \tag{2}$$

where $\tilde{H}(q,p,u)$ is the *pseudo-Hamiltonian* $H_0+\Sigma_{u=1}^m u_iH_i+p_0\Sigma_{i=1}^m u_i^2$, with H_i being defined as $H_i=\langle p,F_i(q)\rangle$, $i=0,1,\cdots,m$. Moreover, an extremal control has to satisfy the maximization condition

$$\tilde{H}(q,p,u)=\max_{v\in\mathbb{R}^m}\tilde{H}(q,p,v), \tag{3}$$

and p_0 is constant and nonpositive. In this situation, one immediately deduces that the maximization condition leads to solve the equation: $\partial\tilde{H}/\partial u=0$ and one must distinguish two cases.

(1) *Normal case*. If $p_0<0$, it can be normalized to $p_0=-1/2$ and solving $\partial\tilde{H}/\partial u=0$ leads to $u_i=H_i$, $i=1,\cdots,m$. Plugging such u_i into $\tilde{H}$ defines a *true Hamiltonian*: $H_n=H_0+\frac{1}{2}\Sigma_{i=1}^m H_i^2$,

whose (smooth) solutions correspond to *normal extremal curves* $z(\cdot)=(q(\cdot),p(\cdot))$, while normal extremal controls are given by $u_i=H_i(z)$, $i=1,\cdots,m$.

(2) *Abnormal case*. It is the situation where $p_0=0$ and hence such extremals have to satisfy the constraints: $H_i=0$, $i=1,\cdots,m$. Such extremals do not depend on the cost and correspond to the so-called *singular trajectories* of the system.[10]

B. Geometric computations of the extremals

We shall complete the computation by introducing adapted geometric coordinates. If $q=(x,y,z)$ are the Cartesian coordinates of the state restricted to the Bloch ball: $|q|\leqslant 1$, using spherical coordinates,

$$x=\rho\sin\phi\cos\theta,\quad y=\rho\sin\phi\sin\theta,\quad z=\rho\cos\phi,$$

the system becomes

$$\dot{\rho}=\gamma_-\cos\phi-\rho(\delta\cos^2\phi+\Gamma),$$

$$\dot{\phi}=-\frac{\gamma_-\sin\phi}{\rho}+\delta\sin\phi\cos\phi+v_2,$$

$$\dot{\theta}=-\cot\phi v_1 \tag{4}$$

where $\delta=\gamma_+-\Gamma$ and the new control $v=v_1+iv_2$ is given by $v=e^{-i\theta}u$. Note, in particular, that the cost is invariant,

$$\int_0^T(v_1^2+v_2^2)dt=\int_0^T(u_1^2+u_2^2)dt.$$

1. Normal extremals in spherical coordinates

Proposition 1: The Hamiltonian H_n associated with normal extremals is given in spherical coordinates by

$$H_n=p_\rho(\gamma_-\cos\phi-\rho(\delta\cos^2\phi+\Gamma))+p_\phi\left(-\frac{\gamma_-}{\rho}\sin\phi+\delta\sin\phi\cos\phi\right)+\frac{1}{2}(p_\phi^2+p_\theta^2\cot^2\phi),$$

where θ is a cyclic variable and p_θ is a first integral.

2. Abnormal extremals in spherical coordinates

Proposition 2: In the case $\delta\neq 0$, an abnormal extremal has to satisfy $p_\phi=0$ and can be

(1) *$\phi=\pi/2$ if $\gamma_-\neq 0$ and $\theta=\theta_0$ constant.*

(2) *$\phi\neq\pi/2$ and corresponds to a singular trajectory of the 2D-system*

$$\dot{y}=-\Gamma y-u_1 z,\quad \dot{z}=\gamma_--\gamma_+z+u_1 z,$$

assuming the control field $u=u_1$ real. It is given in polar coordinates by $\phi=0$ or $2\rho\delta\cos\phi=\gamma_-$, while $p_\theta=0$ is the transversality condition meaning that the θ-variable is not taken into account. The angle θ satisfies: $\dot{\theta}=-\cot\phi v_1$, where v_1 is any control.

C. The analysis in the normal case

The Hamiltonian takes the following form:

$$H_n = \gamma_-\left(p_\rho \cos\phi - \frac{p_\phi}{\rho}\sin\phi\right) + H,$$

where

$$H = -\rho p_\rho(\delta\cos^2\phi + \Gamma) + \frac{1}{2}p_\phi\delta\sin(2\phi) + \frac{1}{2}(p_\phi^2 + p_\theta^2\cot^2\phi).$$

We deduce immediately the following result.

Proposition 3: If $\gamma_-=0$, *the Hamiltonian* H_n *reduces to* H *and is completely integrable. Introducing* $r=\ln\rho$, *it takes the form*

$$H = -p_r(\delta\cos^2\phi + \Gamma) + \frac{1}{2}p_\phi\delta\sin(2\phi) + \frac{1}{2}(p_\phi^2 + p_\theta^2\cot^2\phi),$$

where the set of parameters $\Lambda=(\gamma_+,\Gamma)$ *is such that* $2\Gamma\geqslant\gamma_+\geqslant 0$. *The Hamiltonian is invariant for the central symmetry:* $(p_\phi,\phi)\mapsto(-p_\phi,\pi-\phi)$ *and, moreover, a transformation of the form* $p\mapsto\lambda p$, $\Lambda\mapsto\lambda\Lambda$, $\lambda>0$, *transforms* H *into* λH.

A key property in our analysis is the introduction of a mechanical system. We have

$$\dot\phi = \frac{\partial H_n}{\partial p_\phi} = -\frac{\gamma_-}{\rho}\sin\phi + \frac{1}{2}\delta\sin 2\phi + p_\phi,$$

which leads to

$$H_n = \frac{1}{2}\left(p_\phi + \frac{\delta}{2}\sin(2\phi) - \frac{\gamma_-\sin\phi}{\rho}\right)^2 + \gamma_- p_\rho\cos\phi - \rho p_\rho(\delta\cos^2\phi+\Gamma) + \frac{1}{2}p_\theta^2\cot^2\phi - \frac{1}{2}\left(\frac{\delta\sin 2\phi}{2} - \frac{\gamma_-\sin\phi}{\rho}\right)^2.$$

Hence, we have

Proposition 4: The equation $H_n=h$ *can be written as follows:*

$$\frac{1}{2}\dot\phi^2 + V(\phi) = h,$$

where

$$V = \gamma_- p_\rho\cos\phi - \rho p_\rho(\delta\cos^2\phi+\Gamma) - \frac{1}{2}\left(\delta\frac{\sin(2\phi)}{2} - \frac{\gamma_-\sin\phi}{\rho}\right)^2 + \frac{1}{2}p_\theta^2\cot^2\phi$$

is a potential.

In particular, if $\gamma_-=0$, the potential reduces to

$$V(\phi) = -p_r(\delta\cos^2\phi+\Gamma) - \frac{1}{8}\delta^2\sin^2(2\phi) + \frac{1}{2}p_\theta^2\cot^2\phi.$$

If we set $\psi=\pi/2-\phi$, *one gets*

$$V(\psi) = -p_r(\delta\sin^2\phi+\delta) - \frac{1}{8}\delta^2\sin^2(2\psi) + \frac{1}{2}p_\theta^2\tan^2\psi.$$

Hence, $V(-\psi)=V(\psi)$.

If $\gamma_-=0$, a special case occurs when $\delta=\gamma_+-\Gamma=0$: the ρ-variable cannot be controlled and the energy minimization problem is equivalent to the length minimization problem for the metric $g=d\phi^2+\tan^2\phi d\theta^2$. This metric appears also in the time-minimal control problem since if we parametrize by arc-length, the length corresponds to the time. This control model will play a key role in our analysis.

Definition 1: The quasi-Riemannian metric (with a singularity at the equator) $g=d\phi^2$

$+\tan^2\phi d\theta^2$ is called the standard Grushin metric on the two-sphere of revolution.

Observe that if $\gamma_-=0$, then $V(\phi)\to+\infty$, when $\phi\to 0,\ \pi$, if $p_\theta\neq 0$. This allows one to generalize the Grushin case introducing a one parameter p_r-family of mechanical systems on the two-sphere of revolution which shares the symmetry properties of the Grushin model. The above geometric considerations will lead us to pursue the analysis. First of all, we shall consider the case where $p_\theta=0$, which corresponds to meridian circles in the Grushin model, while $p_\theta\neq 0$ extends the case of extremal curves winding around the equator.

D. Normal extremals in meridian planes

Due to the symmetry of revolution of the problem with respect to the z-axis, we have the following important propositions.

Proposition 5: Extremal curves such that $p_\theta=0$ correspond to extremal curves of the 2D-system:

$$\dot{y}=-\Gamma y-u_1 z,\quad \dot{z}=\gamma_- -\gamma_+ z+u_1 y,$$

where the control u is restricted to the real part u_1 of the control field, the cost being $\int_0^T u_1^2(t)dt$. They give the solutions of the optimal control problem when the initial and final points q_0, q_1 are contained in a same meridian plane.

Proposition 6: If the initial point q_0 of the 3D-system is on the z-axis, then the optimal solution is up to a θ-rotation around the z-axis a solution of the 2D-restricted problem.

1. The integrable case $\gamma_-=0$

The discussion splits into two parts: classification of the phase portraits and parametrization of the extremals.

The Hamiltonian for $p_\theta=0$ reduces to

$$H_n=\gamma_-\left[p_\rho\cos\phi-\frac{p_\phi}{\rho}\sin\phi\right]-\rho p_\rho(\delta\cos^2\phi+\Gamma)+\frac{1}{2}p_\phi\delta\sin(2\phi)+\frac{1}{2}p_\phi^2.$$

If $\gamma_-=0$, introducing $r=\ln\rho$, it takes the form

$$H=-p_r(\delta\cos^2\phi+\Gamma)+\frac{1}{2}(p_\phi\delta\sin(2\phi)+p_\phi^2).$$

Fixing the level set by $H_n=h$ and with $\dot{\phi}=p_\phi+\delta\sin(2\phi)/2$, one gets

$$\frac{1}{2}\dot{\phi}^2+W(\phi)=\bar{h},$$

where $\bar{h}=h+p_r\gamma_+$ and the potential is given by

$$W(\phi)=\frac{\delta^2}{2}\sin^2\phi(\sin^2\phi-a),\quad a=\frac{1}{2}-\frac{p_r}{\delta}.$$

Observe that the system is π-periodic, and the potential function is symmetric: $W(-\phi)=W(\phi)$ and $W(\pi-\phi)=W(\phi)$. Thus, in order to construct the phase portrait of the system, it is enough to analyze the behavior of the function W on the interval $[0,\pi/2]$. The equilibrium points can be determined by the equation

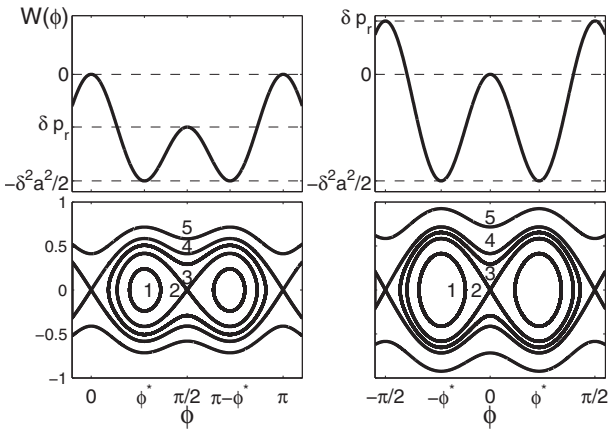

FIG. 1. Phase portraits in the case $a \in]0,1[$ for $\delta p_r < 0$ (left) and $\delta p_r > 0$ (right). In the left panel, numbers 1, 2, 3, 4, and 5 are, respectively, associated with $-\delta^2 a^2/2 < \bar{h} < \delta p_r$, $\bar{h} = \delta p_r$, $\delta p_r < \bar{h} < 0$, $\bar{h} = 0$, and $\bar{h} > 0$. In the right panel, they correspond, respectively, to $-\delta^2 a^2/2 < \bar{h} < 0$, $\bar{h} = 0$, $0 < \bar{h} < \delta p_r$, $\bar{h} = \delta p_r$, and $\bar{h} > \delta p_r$.

$$\frac{\partial W}{\partial \phi} = 2\delta^2 \sin\phi \cos\phi(\sin^2\phi - a) = 0.$$

We get then fixed points $\phi = k\pi/2$ corresponding to the abnormal directions, and in addition, if $a \in]0,1[$, we have one more nontrivial root ϕ_* in the interval $[0, \pi/2]$, which is defined by the relation: $\sin\phi_* = \sqrt{a}$.

To construct the phase portraits, the discussion goes as follows.

Case $a \in]0,1[$*:* We represent the graph of the potential $W(\phi)$. One has $W(0) = 0$ and $W(\pi/2) = \delta^2/2(1-2a) = \delta p_r$. Hence, $W(\pi/2) > 0$ if and only if $p_r \delta > 0$. One gets the two cases displayed in Fig. 1 for $\delta p_r < 0$ and $\delta p_r > 0$. Observe that these phase portraits are identical up to a shift by $\pi/2$. If $p_r = 0$, then $a = \frac{1}{2}$, and hence $\phi_* = \pi/2$. In this critical case, we have the phase portrait of a pendulum with stable equilibria at $\pi/4$, $3\pi/4$, and unstable equilibria at $\phi = 0$, $3\pi/2$ (see Fig. 2).

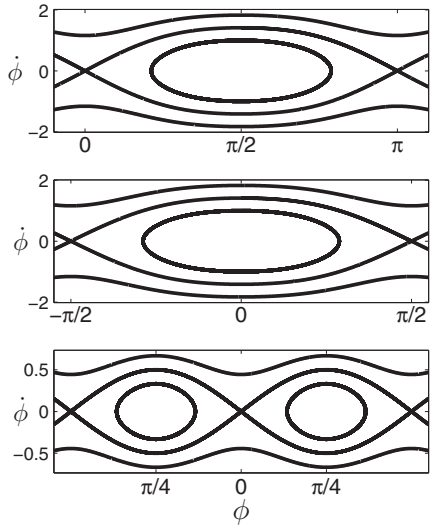

FIG. 2. Phase portraits in the case $a \notin [0,1]$ for $\delta p_r < 0$ (top), $\delta p_r > 0$ (middle), and for $p_r = 0$ (bottom).

Case $a \notin [0,1]$*:* The phase portraits are simpler and correspond to phase portraits of a pendulum where

- if $\delta p_r < 0$, the stable equilibria are at $\pi/2$, $3\pi/2$ and unstable equilibria are at 0, π; and
- if $\delta p_r > 0$, two stable equilibria are at 0, π and unstable equilibria are at $\pi/2$, $3\pi/2$.

Remark 1: From the previous discussion, the mechanical system can be interpreted as a system on the cylinder, identifying 0 and π and this leads to two types of periodic trajectories:

(a) *oscillating trajectories* that are homotopic to zero and
(b) *rotating trajectories* that are not homotopic to zero.

In addition, we have *nonperiodic trajectories* corresponding to separatrices behaviors.

Note that along the first class of trajectories, the angle ϕ oscillates between $\phi_- < \phi_+$, while in the second case in the interval $[0,\pi]$. In this discussion, the abnormal lines correspond to $\phi=0$, $\pi/2$, which are singular points of the normal flow.[10]

To integrate the equations, one can use elliptic integrals. A complete parametrization can be obtained using elliptic functions.[1,29] The computation goes as follows. We have

$$\frac{d\phi}{dt} = \varepsilon\sqrt{2(\bar{h} - W(\phi))}, \quad \varepsilon = \pm 1,$$

and one can consider the branch with $\varepsilon=1$,

$$\dot{\phi} = \sqrt{2(\bar{h} - W(\phi))}.$$

By setting $x=\sin^2\phi$, $\phi \in]0,\pi/2[$, we get

$$dx = 2\sin\phi\cos\phi d\phi$$

and

$$dt = \frac{d\phi}{\sqrt{2(\bar{h} - W(x))}} = \frac{dx}{2\sqrt{2}\sqrt{x(1-x)(\bar{h} - W(x))}}. \tag{5}$$

The parametrization of the solution is related to the roots of the polynomial

$$P(x) = \bar{h} - W(x) = -\frac{\delta^2 x^2}{2} + a\delta^2 x + \bar{h},$$

whose discriminant is

$$\Delta = a^2\delta^4 + 2\delta^2\bar{h} = \delta^2(2\bar{h} + a^2\delta^2).$$

This leads to the following discussion. Consider the case $a \in]0,1[$. According to Fig. 1, nontrivial motion occurs if $\bar{h} > -\delta^2 a^2/2$ and, hence, $\Delta > 0$. The two roots are denoted by $\{x_1, x_2\}$ and their positions with respect to {0, 1} can be deduced from Fig. 1. To get the parametrization, one can use Weierstrass or Jacobi functions. In the first case, we set $y = 1/1-x$ and Eq. (5) takes the form

$$\frac{dx}{2\sqrt{2}\sqrt{x(1-x)(\bar{h} - W(x))}} = \frac{dy}{\sqrt{Q(y)}},$$

where Q is a cubic polynomial whose roots are deduced from the original roots $\{0, x_1, x_2\}$. The integration is then standard.

We shall give the parametrization using the Jacobi functions. Assume that the roots $\{0, 1, x_1, x_2\}$ are ordered as $y_1 > y_2 > y_3 > y_4$ and Eq. (5) is written as

$$\left(\frac{dx}{dt}\right)^2 = 4\delta^2(x-y_1)(x-y_2)(x-y_3)(x-y_4).$$

To conclude the integration we use the transformation from Ref. 20. We set

$$z^2 = \frac{(y_2-y_4)(x-y_3)}{(y_2-y_3)(x-y_4)}.$$

Introducing

$$\Delta_1^2(x) = 4(x-y_1)(x-y_2)(x-y_3)(x-y_4)$$

and

$$\Delta^2(z) = (1-z^2)(1-k^2z^2),$$

we obtain

$$\frac{1}{\Delta(z)}\frac{dz}{dt} = \frac{M}{\Delta_1(x)}\frac{dx}{dt},$$

where

$$k^2 = \frac{(y_2-y_3)(y_1-y_4)}{(y_1-y_3)(y_2-y_4)}, \quad M^2 = \delta^2(y_2-y_3)(y_1-y_3).$$

In this representation, the solution is $z=\mathrm{sn}(Mt+\psi_0,k)$, where z oscillates periodically between -1 and 1 if $0\leqslant k\leqslant 1$ or $-1/k$, $1/k$ if $k\geqslant 1$, with k being the modulus. According to our parametrization, when x oscillates between y_2 and y_3, z^2 oscillates between 0 and 1, and the parameter $k \in [0,1]$.

The x-variable can be found by inverting the Möbius transformation

$$x = \frac{z^2(y_2-y_3)y_4 - (y_2-y_4)y_3}{z^2(y_2-y_3) - (y_2-y_4)}.$$

If the initial condition $x(0)=x_0$ is fixed by $x_0=\sin^2\phi(0)$, then $z(t)=\mathrm{sn}(\delta Mt+\psi_0,k)$, with ψ_0 defined by $z(0)=\mathrm{sn}(\psi_0,k)$.

The integration of the remaining equation

$$\dot{r} = -\delta\cos^2\phi - \gamma_+ = \delta x - \gamma_+$$

leads to an expression of the form

$$r(t) = -\gamma_+ t + \int \frac{a+b\,\mathrm{sn}^2 u}{c+d\,\mathrm{sn}^2 u}du,$$

where a, b, c, and d are constants that can be expressed in terms of δ, x_1, and x_2. The integral term can be computed using elliptic integrals of the third kind.[29] Indeed,

$$\int \frac{a+b\,\mathrm{sn}^2 u}{c+d\,\mathrm{sn}^2 u}du = \frac{a}{c}u + \frac{(bc-ad)}{c^2}\int \frac{\mathrm{sn}^2 u}{1+e\,\mathrm{sn}^2 u}du, \tag{6}$$

where $e=d/c$. Defining the complex parameter $\bar{a}$ by the equation

$$\mathrm{sn}^2\,\bar{a} = -\frac{e}{k^2},$$

the last term of (6) can be found using the standard form of the elliptic integral of the third kind

$$\Pi(u,\bar{a},k)=\int_0^u \frac{k^2\,\mathrm{sn}\,\bar{a}\,\mathrm{cn}\,\bar{a}\,\mathrm{dn}\,\bar{a}\,\mathrm{sn}^2\,v}{1-k^2\,\mathrm{sn}^2\,\bar{a}\,\mathrm{sn}^2\,v}dv\,.$$

Applying the previous techniques, one gets the following parametrizations.

- Short orbits $-\delta^2a^2/2<\bar{h}<\delta p_r<0$ or $-\delta^2a^2/2<\bar{h}<0<\delta p_r$.

  We have $0<x_1<x_2<1$. Then

$$x(t)=\frac{x_1x_2}{x_2-(x_2-x_1)\mathrm{sn}^2(Mt+\psi_0,k)},$$

$$r(t)=\frac{\delta x_1}{M}\left(\Pi\left(\frac{x_2-x_1}{x_2},\mathrm{am}(Mt+\psi_0,k),k\right)-\Pi\left(\frac{x_2-x_1}{x_2},\mathrm{am}(\psi_0,k),k\right)\right)-\gamma_+t,$$

  where

$$M^2=\delta^2x_2(1-x_1),\quad k^2=\frac{x_2-x_1}{x_2(1-x_1)}.$$

- Long orbits $\delta p_r<\bar{h}<0$.

  In this case $0<x_1<1<x_2$, and

$$x(t)=\frac{x_1}{1-(1-x_1)\mathrm{sn}^2(Mt+\psi_0,k)},$$

$$r(t)-r(0)=\frac{\delta x_1}{M}(\Pi(1-x_1,\mathrm{am}(Mt+\psi_0,k),k)-\Pi(1-x_1,\mathrm{am}(\psi_0,k),k))-\gamma_+t,$$

  where

$$M^2=\delta^2(x_2-x_1),\quad k^2=\frac{x_2(1-x_1)}{x_2-x_1}.$$

- Long orbits $0<\bar{h}<\delta p_r$. This case is analog to the previous one up to the shifting along the ϕ-axis. More precisely, we have $x_1<0<x_2<1$, and

$$x(t)=1-\frac{1-x_2}{1-x_2\,\mathrm{sn}^2(Mt+\psi_0,k)},$$

$$r(t)-r(0)=-\frac{\delta(1-x_2)}{M}(\Pi(x_2,\mathrm{am}(Mt+\psi_0,k),k)-\Pi(x_2,\mathrm{am}(\psi_0,k),k))-\Gamma t$$

  for M and k as in the previous case.
- Rotating motions $\delta p_r<0<\bar{h}$ or $0<\delta p_r<\bar{h}$.

  We have $x_1<0<1<x_2$. We set

$$M^2 = \delta^2 x_2(1-x_1), \quad k^2 = \frac{x_2 - x_1}{x_2(1-x_1)}.$$

Then

$$x(t) = \frac{x_1 \,\mathrm{sn}^2(Mt + \psi_0, k)}{\mathrm{sn}^2(Mt + \psi_0, k) - 1 + x_1},$$

$$r(t) - r(0) = -\frac{\delta x_1}{M}\left(\Pi\left(\frac{1}{1-x_1}, \mathrm{am}(Mt+\psi_0,k), k\right) - \Pi\left(\frac{1}{1-x_1}, \mathrm{am}(\psi_0,k), k\right)\right) + (-\gamma_+ t + \delta x_1)t.$$

2. The general case $\gamma_- \neq 0$

In this section, we shall interpret the effect of $\gamma_- \neq 0$ on the set of extremals. Using polar coordinates, the mechanical system takes the form

$$\frac{\dot{\phi}^2}{2} + V(\phi, p_r, r) = h,$$

where

$$V(\phi, p_r, r) = p_r[\gamma_- \cos\phi e^{-r} - (\Gamma + \delta\cos^2\phi)] - \frac{1}{2}\left[\frac{\delta \sin(2\phi)}{2} - \gamma_- \sin\phi e^{-r}\right]^2.$$

Since $\gamma_- \neq 0$, we have a coupling between the evolution of the ϕ- and r-variables which can be interpreted as a *true dissipation effect* on the set of extremals. In order to make the analysis, we use Cartesian coordinates which allow to make a Poincaré compactification to analyze the ω-limit set. The Hamiltonian becomes

$$H_n = -\Gamma y p_y + p_z(\gamma_- - \gamma_+ z) + \frac{1}{2}(y p_z - z p_y)^2.$$

Introducing

$$P = y p_z - z p_y, \quad Q = y p_y + z p_z$$

the extremal system is

$$\dot{y} = -\Gamma y - zP,$$

$$\dot{z} = (\gamma_- - \gamma_+ z) + yP,$$

$$\dot{p}_y = \Gamma p_y - p_z P,$$

$$\dot{p}_z = \gamma_+ p_z - p_z P,$$

and the Poincaré compactification is

$$\dot{y} = -\Gamma y w^2 + z(z p_y - y p_z),$$

$$\dot{z} = \gamma_- w^3 - \gamma_+ w^2 z + y(y p_z - z p_y),$$

$$\dot{p}_y = \Gamma p_y w^2 + p_z(zp_y - yp_z),$$

$$\dot{w} = 1.$$

The quantities P, Q corresponding to dual polar coordinates can be used as coordinates provided that $p_y^2+p_z^2 \neq 0$. We have

$$\dot{Q} = \gamma_- p_z,$$

$$\dot{P} = \delta(yp_z + zp_y) - \gamma_- p_y.$$

The equilibrium points can be easily computed. If $\gamma_- \neq 0$, one has $p_z=0$. Hence, $\dot{p}_y=0$ gives $p_y=0$ if $\Gamma \neq 0$. If $\dot{y}=0$, then $y=0$ and if $\dot{z}=0$, one has $z=\gamma_-/\gamma_+$. This corresponds to the equilibrium point of the free motion. Additional critical points can occur at the infinity. Indeed, due to the dissipation, Poisson-stable point does not exist and from Hopf theorem almost every point is departing.[35] Since the state variables remain bounded, we deduce that the adjoint vector $|p| \to \infty$ as $t \to +\infty$. This can be made more precise using the following transformation:

$$p_y = \varrho \cos \vartheta, \quad p_z = \varrho \sin \vartheta,$$

with

$$\varrho\dot{\varrho} = \Gamma p_y^2 + \gamma_+ p_z^2$$

and

$$\Gamma p_y^2 + \gamma_+ p_z^2 \geqslant \gamma_+ \varrho^2/2$$

since $2\Gamma \geqslant \gamma_+ \geqslant 0$. Hence, in particular, $\varrho(t) \geqslant e^{\gamma_+ t/2}\varrho(0)$ and this gives $|p| \to +\infty$ if $t \to +\infty$, provided that $\varrho(0) \neq 0$. We also have

$$\dot{\vartheta} = \frac{\delta \sin(2\vartheta)}{2} + P.$$

To summarize, we obtain

$$\dot{\varrho} = \varrho(\Gamma + \delta \sin^2 \vartheta),$$

$$\dot{\vartheta} = \delta \sin(2\vartheta)/2 + P,$$

$$\dot{P} = \delta[\sin(2\vartheta)Q - \cos(2\vartheta)P] - \gamma_- \varrho \cos \vartheta,$$

$$\dot{Q} = \gamma_- \varrho \sin \vartheta.$$

It is a convenient coordinate system if $\varrho \neq 0$. In this representation P is the control and numerical simulations can be used to analyze the limit behaviors of P and Q. This gives a complete classification of the extremal curves in meridian planes.

E. Normal extremals in nonmeridian planes

We now proceed to the analysis of normal extremals such that $p_\theta \neq 0$. As before, we distinguish the two cases.

1. The integrable case $\gamma_-=0$

Fixing the level set to $H=h$, one can reduce the integration to find the solutions of $\dot{\phi}^2/2 + V(\phi)=h$, while the remaining equations are

$$\dot{\theta}=p_\theta\left(\frac{1}{\sin^2\phi}-1\right), \quad \dot{r}=-\delta\sin^2\phi-\gamma_+.$$

We introduce in this section the following notations:

$$b=\Gamma-\gamma_+, \quad a=\frac{1}{2}+\frac{p_r}{b}, \quad \bar{h}=h+p_r\gamma_++\frac{p_\theta^2}{2}.$$

If we denote $x=\sin^2\phi$, we obtain

$$V(\phi)=\widetilde{V}(x)=\frac{b^2}{2x}\left(x^3-2ax^2+\frac{p_\theta}{b^2}\right)-p_r\gamma_+-\frac{p_\theta^2}{2}$$

and introducing

$$W(x)=\frac{b^2}{2x}\left(x^3-2ax^2+\frac{p_\theta^2}{b^2}\right),$$

one deduces that ϕ satisfies the equation

$$\dot{\phi}=\pm\sqrt{2(\bar{h}-W(x(\phi)))}.$$

Step 1: Qualitative analysis of the potential function W. Since $x=\sin^2\phi$, $x\in[0,1]$ but we extend the domain to the whole $\mathbb{R}$. First of all we observe that

$$\lim_{x\to\pm 0}W(x)=\pm\infty, \quad \lim_{x\to\pm\infty}W(x)=+\infty$$

and

$$W(1)=-bp_r+\frac{p_\theta^2}{2}.$$

Further, we have

$$W'_x=\frac{b^2}{x^2}\left(x^3-ax^2-\frac{p_\theta^2}{2b^2}\right).$$

Hence, $\lim_{x\to 0}W'_x=\infty$ and the critical points of W are defined by the roots of the cubic polynomial

$$P_1(x)=x^3-ax^2-\frac{p_\theta^2}{2b^2}.$$

Since $P_1(0)=-p_\theta^2/2b^2\leqslant 0$ and $P_1'(0)=0$, if $p_\theta\neq 0$, the polynomial $P_1(x)$ has one positive real root x_*, and the other possible real roots of P_1 (at most two) are negative. In particular, it follows that $W(x)$ can have at most one critical point on $]0,1[$. This is explained in the next section.

By construction, the critical point x_* is a positive zero of the function W', and thus it solves the following equation:

$$b^2x - ab^2 = \frac{p_\theta^2}{2x^2}.$$

It is then easy to see that in the domain $x \geqslant 0$, the graph of the linear function $f_1 = b^2x - ab^2$ intersects the graph of $f_2 = \frac{1}{2}p_\theta^2 x^{-2}$ only once, and the intersection point $x_* < 1$ if and only if $f_1(1) > f_2(1)$. This yields the following condition:

$$a < 1 - \frac{p_\theta^2}{2b^2}$$

or, equivalently,

$$p_\theta^2 - 2p_r\delta < \delta^2.$$

Now consider the potential $\tilde{W}(\phi) = W(x(\phi))$. We have

$$\tilde{W}'(\phi) = 2W'(x(\phi))\sin\phi\cos\phi,$$

hence $\tilde{W}'(\pi/2) = 0$. Taking into account the symmetry of the function $\tilde{W}$ with respect to the equator $\phi = \pi/2$, we finally obtain two cases accordingly to the values of the dissipative parameters Γ, γ_+ and the first integrals p_r and p_θ.

Type I: $a < 1 - p_\theta^2/2b^2$, then $x_* < 1$. The motion of the system takes place in the region $\bar{h} \geqslant W(x_*)$. There are three equilibrium states

$$\phi_{*0} = \frac{\pi}{2},$$

corresponding to a local maximum of the potential and

$$\phi_{*1} = \arcsin\sqrt{x_*}, \quad \phi_{*2} = \pi - \arcsin\sqrt{x_*},$$

corresponding to a local minimum of the potential. They belong, respectively, to the energy levels $W(1)$ and $W(x_*)$. There are two types of periodical trajectories: to each value $W(x_*) < \bar{h} < W(1)$ corresponds two periodic orbits in each hemisphere which are symmetric with respect to the equator, and for $\bar{h} > W(1)$, there exists a unique periodic orbit crossing the equatorial plane $\phi = \pi/2$ and the two pieces are symmetric with respect to the equator. The transition between the two cases gives a limit situation which is nonperiodic and corresponds to a separatrix on the energy level $\bar{h} = W(1)$.

Type II: $a \geqslant 1 - p_\theta^2/2b^2$. In this case the motion of the system takes place in the region $h \geqslant W(1)$ and there exists a unique equilibrium state $\phi_{*0} = \pi/2$. The only type of periodic orbits crossing the equatorial plane corresponds to the energy levels $\bar{h} > W(1)$. Those orbits can be identified with the analogous orbits of Case I. This leads to the following definition.

Definition 2: For the generic motion of the mechanical system $\dot{\phi}^2/2 + V(\phi) = h$, we have two types of periodic orbits: orbits located in one hemisphere, called short orbits, and orbits crossing the equators, called long orbits.

Step 2: Parametrization of the extremal trajectories by elliptic functions. The ϕ-variable is solution of

$$\dot{\phi} = \pm\sqrt{2(\bar{h} - \tilde{W}(\phi))},$$

where the $\pm$ represents the ascending and descending branches. It is not restrictive to consider the case $\dot{\phi} > 0$. From the previous discussion, it is sufficient to analyze the equation in the x-variable, $x = \sin^2\phi$. Then we can consider

$$dt = \frac{d\phi}{\sqrt{2(\bar{h} - \tilde{W}(\phi))}} = \frac{dx}{2\sqrt{2}\sqrt{x(1-x)(\bar{h} - W(x))}}$$

and

$$x(\bar{h} - W(x)) = -\frac{b^2}{2}\left(x^3 - 2ax^2 - \frac{2\bar{h}}{b^2}x + \frac{p_\theta^2}{b^2}\right) = -\frac{b^2}{2}P_2(x),$$

where $P_2(x)$ is the cubic polynomial,

$$P_2(x) = x^3 - 2ax^2 - \frac{2\bar{h}}{b^2}x + \frac{p_\theta^2}{b^2}$$

and we have

$$\frac{dx}{2\sqrt{2}\sqrt{x(1-x)(\bar{h} - W(x))}} = \frac{dx}{2|b|\sqrt{(x-1)P_2(x)}}.$$

In order to characterize the roots of the polynomial P_2, we have to consider two cases.

Case a: $\bar{h} < W(1)$ (short orbits). We have

$$P_2(0) = \frac{p_\theta^2}{b^2} > 0, \quad P_2(1) = \frac{2}{b^2}(W(1) - \bar{h}) > 0.$$

According to the shape of the potential, the function $\bar{h} - W(x)$ and, hence, the polynomial $P_2(x)$ has exactly

- two roots $0 < x_1 < x_2 < 1$ in the interval $]0,1[$ if $W(1) > \bar{h} > W(x_*)$,
- no root if $\bar{h} < W(x_*)$, and
- short orbits reduce to equilibrium states if $\bar{h} = W(x_*)$.

In addition, since $P_2(x) \to -\infty$ as $x \to -\infty$, one can deduce that P_2 necessarily has a negative root $x_3 < 0$.

Case b: $\bar{h} > W(1)$ (long orbits). We have

$$P_2(0) = \frac{p_\theta^2}{b^2} > 0, \quad P_2(1) = \frac{2}{b^2}(W(1) - \bar{h}) < 0.$$

Taking into account that $P_2(x)$ has at most one extremum at $0 < x_* < 1$, we deduce that $P_2(x)$ has exactly two positive roots x_1, x_2 and a negative root x_3 so that $x_3 < 0 < x_1 < 1 < x_2$.

Summing up, we get that in both cases

$$(1-x)x(\bar{h} - W(x)) = \frac{b^2}{2}(x - y_1)(x - y_2)(x - y_3)(x - y_4),$$

where the real roots are ordered according to $y_1 > y_2 > y_3 > y_4$. To integrate, we proceed as before to get the following parametrization.

Parametrization of periodic orbits. We proceed as in Sec. II D. We have to integrate the following equation:

$$dt = \frac{dx}{2|b|\sqrt{(x-1)(x-x_1)(x-x_2)(x-x_3)}}. \tag{7}$$

According to our previous analysis, in terms of x-variable the motion occurs in the interval $[x_1, \min\{x_2, 1\}]$. The change of variables

$$z^2 = \frac{(\min\{x_2,1\}-x_3)(x_1-x)}{(\ \min\{x_2,1\}-x_1))(x_3-x)}$$

transforms the right-hand side of (7) into the following form:

$$\sqrt{b^2(\max\{1,x_2\}-x_1)(\min\{1,x_2\}-x_3)}dt = \frac{dz}{\sqrt{(1-z^2)(1-k^2z^2)}},$$

where

$$k^2 = \frac{(\max\{1,x_2\}-x_3)(\min\{1,x_2\}-x_1)}{(\min\{1,x_2\}-x_3)(\max\{1,x_2\}-x_1)}.$$

Integrating with $z(t)=0$ for $t=0$, we get

$$z(t) = \mathrm{sn}(Mt,k),$$

where

$$M = \sqrt{b^2(\max\{1,x_2\}-x_1)(\min\{1,x_2\}-x_3)}.$$

The x-variable can be found as

$$x(t) = \frac{-x_1(\min\{1,x_2\}-x_3)+x_3(\min\{1,x_2\}-x_1)z^2(t)}{-(\min\{1,x_2\}-x_3)+x_3(\min\{1,x_2\}-x_1)z^2(t)},$$

with the corresponding initial condition deduced from $z(0)=0$. The general case can be obtained using a proper time shift.

Taking into account the position of the roots x_i, we get the following parametrization of the periodic orbits.

Short orbits. We have $\min\{1,x_2\}=x_2$, $\max\{1,x_2\}=1$. Thus,

$$k^2 = \frac{(1-x_3)(x_2-x_1)}{(x_2-x_3)(1-x_1)}, \quad M = \sqrt{\delta^2(1-x_1)(x_2-x_3)},$$

$$\phi(t) = \arcsin\left[\frac{-x_1(x_2-x_3)+x_3(x_2-x_1)z^2(t)}{-(x_2-x_3)+x_3(x_2-x_1)z^2(t)}\right],$$

while the remaining variables are given by

$$\theta(t)-\theta(0) = \frac{(1-x_3)p_\theta t}{x_3} + \frac{p_\theta(x_3-x_1)}{x_1x_3M}\Pi\left(\frac{x_3(x_2-x_1)}{x_1(x_2-x_3)}, \mathrm{am}(Mt,k), k\right),$$

$$r(t)-r(0) = (\delta x_3+\gamma_+)t + \frac{\delta(x_1-x_3)}{M}\Pi\left(\frac{x_2-x_1}{x_2-x_3}, \mathrm{am}(Mt,k), k\right).$$

Long orbits. We have $\min\{1,x_2\}=1$, $\max\{1,x_2\}=x_2$,

$$k^2 = \frac{(x_2 - x_3)(1 - x_1)}{(1 - x_3)(x_2 - x_1)}, \quad M = \sqrt{\delta^2 (x_2 - x_1)(1 - x_3)}.$$

The long orbits cross the equatorial plane and ϕ has to be prolongated analytically using either arcsin or $\pi - \arcsin$. For θ and r, we get

$$\theta(t) - \theta(0) = \frac{(1 - x_3) p_\theta t}{x_3} + \frac{p_\theta (x_3 - x_1)}{x_1 x_3 M} \Pi\left(\frac{x_3 (1 - x_1)}{x_1 (1 - x_3)}, \mathrm{am}(Mt, k), k \right),$$

$$r(t) - r(0) = (\delta x_3 + \gamma_+) t + \frac{\delta (x_1 - x_3)}{M} \Pi\left(\frac{1 - x_1}{1 - x_3}, \mathrm{am}(Mt, k), k \right).$$

To get a complete parametrization for $p_\theta \neq 0$, one must add

(a) trajectories such that $\phi(t)$ is reduced to a single point. If we represent the corresponding trajectory $(\phi(t), \theta(t))$ on the two-sphere, they will form the so-called *parallel solutions*.
(b) The transitions between short and long periodic orbits correspond in the ϕ-variable to *separatrices*. They can be obtained as limit cases for the two families of periodic orbits since $\lim_{k \to 1} \mathrm{sn}(u, k) = \tanh u$.

Remark 2: This computation can be compared with the Grushin case for which there exists only one type of periodic orbits, all in the long category. Also the transcendence is different since one needs only elementary functions in the Grushin case.

Remark 3: One important information concerning the ϕ-parametrization is the amplitude of the oscillations and the period computation.

2. Analysis in the case $\gamma_- \neq 0$

In this case, using the coordinates (r, ϕ, θ), $r = \ln \rho$, $\rho \in]0, 1]$, $r \in]-\infty, 0]$, the system takes the form

$$\dot{r} = \gamma_- \cos \phi e^{-r} - (\delta \cos^2 \phi + \Gamma),$$

$$\dot{\phi} = -\gamma_- \sin \phi e^{-r} + \delta \sin \phi \cos \phi + v_2,$$

$$\dot{\theta} = -\cot \phi v_1,$$

and the extremal controls are $v_2 = p_\phi$ and $v_1 = p_\theta \cot \phi$ and taking the controls in $L^2[0, T]$, one gets the condition $\int_0^T (p_\phi^2 + p_\theta^2 \cot^2 \phi) dt < +\infty$.

Recall that the equilibrium point of the free motion is given in Cartesian coordinates by

$$x = y = 0, \quad z = \frac{\gamma_-}{\gamma_+},$$

and in spherical coordinates by

$$\rho = \frac{|\gamma_-|}{\gamma_+}, \quad \phi = 0 \quad \text{if } \gamma_- > 0, \quad \phi = \pi \quad \text{if } \gamma_- < 0.$$

Since $\int_0^T (p_\phi^2 + p_\theta^2 \cot^2 \phi) dt < +\infty$, the condition $\phi \to 0, \pi$ on $[0, T]$ is excluded if $p_\theta \neq 0$. The Hamiltonian is

$$H = p_r [\gamma_- \cos \phi e^{-r} - (\delta \cos^2 \phi + \Gamma)] + p_\phi \left[-\gamma_- \sin \phi e^{-r} + \frac{\delta}{2} \sin(2\phi) \right] + \frac{1}{2} (p_\phi^2 + p_\theta^2 \cot^2 \phi).$$

We have

$$\dot{\phi} = \frac{\partial H}{\partial p_\phi} = -\gamma_- e^{-r} \sin\phi + \frac{\delta}{2}\sin(2\phi) + p_\phi,$$

hence,

$$p_\phi = \dot{\phi} + \gamma_- e^{-r} \sin\phi - \delta \sin\phi \cos\phi.$$

The Hamiltonian is written as

$$H = p_r[\gamma_- \cos\phi e^{-r} - (\delta\cos^2\phi + \Gamma)] + \frac{1}{2}(p_\phi - \gamma_- e^{-r}\sin\phi + \delta\sin\phi\cos\phi)^2 + \frac{1}{2}p_\theta^2\cot^2\phi$$
$$- \frac{1}{2}(\delta\sin\phi\cos\phi - \gamma_- e^{-r}\sin\phi)^2.$$

Hence, one gets

$$\frac{1}{2}\dot{\phi}^2 + V(\phi, r, p_r) = h,$$

where the potential is now

$$V = p_r[\gamma_- \cos\phi e^{-r} - (\delta\cos^2\phi + \Gamma)] - \frac{1}{2}(\delta\sin\phi\cos\phi - \gamma_- e^{-r}\sin\phi)^2 + \frac{1}{2}p_\theta^2\cot^2\phi.$$

The first step is to analyze the effect of γ_- on the parallel extremals occurring when $\gamma_- = 0$. That is, one must find the singular point solutions of the following system:

$$\dot{r} = \frac{\partial H}{\partial p_r} = \gamma_- e^{-r}\cos\phi - (\delta\cos^2\phi + \Gamma),$$

$$\dot{p}_r = -\frac{\partial H}{\partial r} = \gamma_- e^{-r}(p_r\cos\phi - p_\phi\sin\phi),$$

$$\dot{\phi} = \frac{\partial H}{\partial p_\phi} = -\gamma_- e^{-r}\sin\phi + \frac{\delta}{2}\sin(2\phi) + p_\phi,$$

$$\dot{p}_\phi = -\frac{\partial H}{\partial \phi} = [\gamma_- e^{-r}\sin\phi - 2\delta\cos\phi\sin\phi]p_r - p_\phi(-\gamma_- e^{-r}\cos\phi + \delta\cos(2\phi)) + p_\theta^2\frac{\cos\phi}{\sin^3\phi}.$$

Hence, for $e^{-r} \neq 0$, we must solve

$$\gamma_- e^{-r}\cos\phi - (\delta\cos^2\phi + \Gamma) = 0,$$

$$p_r\cos\phi - p_\phi\sin\phi = 0,$$

$$p_\phi = \gamma_- e^{-r}\sin\phi - \frac{\delta}{2}\sin(2\phi),$$

$$p_r[\gamma_- e^{-r}\sin\phi - \delta\sin(2\phi)] + p_\phi(\gamma_- e^{-r}\cos\phi - \delta\cos(2\phi)) + p_\theta^2\frac{\cos\phi}{\sin^3\phi} = 0.$$

One gets

$$\gamma_- e^{-r} = \frac{\delta \cos^2 \phi + \Gamma}{\cos \phi},$$

$$p_r = p_\phi \tan \phi,$$

$$p_\phi = \gamma_- e^{-r} \sin \phi - \frac{\delta}{2} \sin(2\phi),$$

and replacing in the last equation, we obtain

$$\tan^3 \phi(\delta \cos^2 \phi + \Gamma)^2 - \frac{3}{2} \tan^2 \phi(\delta \cos^2 \phi + \Gamma)\delta \sin(2\phi) + \tan \phi \frac{\delta^2}{2} \sin^2(2\phi) + \tan \phi(\delta \cos^2 \phi + \Gamma)^2 - \tan \phi(\delta \cos^2 \phi + \Gamma)\delta \cos(2\phi) - \frac{\delta}{2} \sin(2\phi)(\delta \cos^2 \phi + \Gamma) + \frac{\delta^2}{2} \sin(2\phi)\cos(2\phi) + p_\theta^2 \frac{\cos \phi}{\sin^3 \phi} = 0.$$

We have to solve

$$\frac{P(\phi)}{\sin^3 \phi \cos^3 \phi} = 0,$$

where

$$P(\phi) = \sin^6 \phi(\delta \cos^2 \phi + \Gamma)^2 - \frac{3}{2} \sin^5 \phi \cos \phi(\delta \cos^2 \phi + \Gamma)\delta \sin(2\phi) + \sin^4 \phi \cos^2 \phi \frac{\delta^2}{2} \sin^2(2\phi) + \sin^4 \phi \cos^2 \phi(\delta \cos^2 \phi + \Gamma)^2 - \sin^4 \phi \cos^2 \phi(\delta \cos^2 \phi + \Gamma)\delta \cos(2\phi) - \sin^3 \phi \cos^3 \phi \frac{\delta}{2} \sin(2\phi)(\delta \cos^2 \phi + \Gamma) + \sin^3 \phi \cos^3 \phi \frac{\delta^2}{2} \sin(2\phi)\cos(2\phi) + p_\theta^2 \cos^4 \phi = 0.$$

Again, setting $x = \sin^2 \phi$, one observes that $P(x) = 0$ is a polynomial equation of *degree 6* where P can be written after simplification as

$$P(x) = (x-1)^2(p_\theta^2 - 2\delta^2 x^4) + \Gamma^2 x^2.$$

An analysis of the polynomial P leads to the following result.

Proposition 7: The polynomial P has no root in the interval $[0, 1]$ *for any values of the parameters* p_θ, Γ, *and* δ *satisfying the constraint* $2\Gamma \geqslant \gamma_+$.

Proof: We construct a polynomial Q such that $P(x) \geqslant Q(x)$ for $x \in [0, 1]$. Since $2\Gamma \geqslant \gamma_+$ and $\delta = \gamma_+ - \Gamma$, one deduces that $\delta \leqslant \Gamma$. We also use the fact that the polynomial $(x-1)^2 x^2$ reaches its maximum for $x = 1/2$ in the interval $[0, 1]$. One then arrives at $Q(x) = (x-1)^2 p_\theta^2 + \frac{7}{8}\Gamma^2 x^2$, which is strictly positive for nonzero values of p_θ and Γ. □

Using Proposition 7, it is then straightforward to show that there exist no parallel extremal in the case $\gamma_- \neq 0$.

To complete the analysis, we proceed as in Sec. II D. Again Hopf theorem can be used to prove that the adjoint vector $p(\cdot)$ is not bounded when $t \to +\infty$. However it can be directly seen using adapted coordinates. We introduce the following notations:

$$P = yp_z - zp_y, \quad Q = zp_x - xp_z, \quad R = xp_y - yp_x,$$

and the adjoint vector is represented in polar coordinates

$$p_x = \varrho \sin\varphi \cos\psi, \quad p_y = \varrho \sin\varphi \sin\psi, \quad p_y = \rho \cos\varphi.$$

Computing, one gets

$$\dot{\varrho} = \varrho(\Gamma \sin^2\varphi + \gamma_+ \cos^2\varphi),$$

$$\dot{\psi} = -\frac{\sin(2\varphi)}{2}(P\cos\psi + Q\sin\psi),$$

$$\dot{\varphi} = -\frac{\delta \sin(2\varphi)}{2} + (Q\sin\psi - P\sin\psi),$$

where P and Q represent the control components. They satisfy the following equations:

$$\dot{P} = \delta(yp_z + zp_y) + QR - p_y\gamma_-,$$

$$\dot{Q} = p_x\delta - \delta(p_xz + p_zx) - PR,$$

and, moreover, $\dot{R}=0$. The state variables are solutions of

$$\dot{x} = -\Gamma x + zQ,$$

$$\dot{y} = -\Gamma y - zP,$$

$$\dot{z} = (\gamma_- - \gamma_+ z) + yP - xQ.$$

In particular, one deduces that $\dot{\varrho} \geqslant \gamma_+\varrho/2$ and $\varrho(t) \geqslant e^{\gamma_+ t/2}\varrho(0)$. Hence, $\varrho(t) \to +\infty$ when $t \to +\infty$ if $\varrho(0) \neq 0$. Again the Poincaré compactification allows one to study the asymptotic behaviors. Due to the complexity of the equations, it has to be numerically analyzed.

III. THE OPTIMALITY PROBLEM

A crucial step in our analysis is to determine the optimality status of extremal curves since the maximum principle is only a necessary optimality condition. In order to get second order necessary and sufficient optimality conditions under generic assumptions, the basic problem is to compute the conjugate points. This is the main discussion of this section, in relation to the classification of extremals and the determination of the value function, solution of the Hamilton–Jacobi–Bellman equation.

A. Existence theorem

The standard existence theorem can be applied.[30] Indeed, the system can be written in the form

$$\dot{q}(t) = Aq(t) + Bq(t)u(t), \quad q(0) = q_0$$

with cost integral $\int_0^T |u|^2 dt$, the class of admissible controls being the set $L^2[0,T]$,

$$\int_0^T |u|^2 dt < +\infty.$$

Since the dynamics is bilinear, the method of variation of the constant leads to a system of the form: $\dot{y}(t) = (C(t)y(t))u(t)$, $y(0) = y_0$ for which we deduce immediately the bound

$$|y(t)| \leqslant \beta(|u|_{L^1[0,T]}),$$

where β is monotone increasing. Another remark is that in the application of the maximum principle, we can extend the class of admissible control from $L^\infty[0,T]$ to $L^2[0,T]$ since we apply only the weak version, the extremal curves corresponding to the singularity of the end-point mapping. We can replace in the computation of the Fréchet derivative the L^∞-norm by the L^2-norm.[10] This leads to the following properties.

Proposition 8: For the system (1) restricted to the Bloch ball $|q| \leqslant 1$, *for each pair of points* q_0, q_1 *such that* q_0 *can be steered to* q_1, *there exists an optimal control* u^* *minimizing the cost. Moreover, the optimal solutions are extremal curves, solutions of the maximum principle*.

Remark 4: See also Ref. 24 for another proof.

B. Optimality concepts

Before analyzing the optimality, it is important to introduce the following geometric objects, which are related to standard Riemannian geometry.[21] We shall restrict our analysis to normal extremals only, for reasons which will be clarified later.

Definition 3: We recall that normal extremals are solutions of the smooth Hamiltonian vector field $\vec{H}_n$ and let $\exp[t\vec{H}_n]$ be the one parameter group. We denote by $z(t)=(q(t),p(t))$, $t \in [0,T]$ a reference extremal. If we fix $q(0)=q_0$, the *exponential mapping* is the map

$$\exp_{q_0,t}: p(0) \mapsto \Pi[\exp t\vec{H}_n(q_0,p(0))],$$

where II: $(q,p) \mapsto q$ is the standard projection. The time t_c is said *conjugate* if the exponential mapping is not immersive at $t=t_c$ and we note t_{1c} the first conjugate time, with corresponding first conjugate point $q(t_{1c})$. The point $q(t)$, along the reference extremal, is said a *separating point* if there exists another extremal curve $z'(\cdot)=(p'(\cdot),q'(\cdot))$ with $q(\cdot)$ and $q'(\cdot)$ distinct such that $q(t)=q'(t)$ and q and q' have the same cost on $[0,t]$. The *cut point* along the reference extremal is the first point $q(t_{cc})$ such that $q(\cdot)$ is no more optimal, beyond the time t_{cc}. Fixing the final time to T, the set of such points when considering all the extremal curves will form, respectively, the *conjugate locus* $C(q_0)$, the *separating locus* $L(q_0)$ and the *cut locus* $C_{ut}(q_0)$.

C. Symmetries and optimality

Using the discrete symmetric group on the set of extremals, we can immediately compute obvious separating points.

1. The integrable case

Consider the case $\gamma_-=0$ and $p_\theta \neq 0$. The relation $H_n=h$ gives

$$\frac{1}{2}\dot{\phi}^2 + V(\phi) = h,$$

where the potential is

$$V(\phi) = -p_r(\delta\cos^2\phi + \Gamma) - \frac{1}{8}\delta^2\sin^2(2\phi) + \frac{1}{2}p_\theta^2\cot^2\phi.$$

We fix p_θ and p_r and for each initial condition $\phi(0)$, we have two extremal curves on the level set h, starting, respectively, from $\dot{\phi}(0)$ and $-\dot{\phi}(0)$. They are distinct and periodic if and only if $\dot{\phi}(0) \neq 0$ and the level set is without equilibrium point (for the fixed values of p_r and p_θ). If T is the corresponding period, we immediately deduce the following.

Proposition 9: For fixed p_r *and* p_θ, *the two periodic extremal curves starting from* $\phi(0)$, $\dot{\phi}(0) \neq 0$ *and with the same* $\theta(0)$, $r(0)$ *intersect at the same point, with the same cost, after one period T. Hence, the corresponding point belongs to the separating locus.*

Moreover, we have the following.

Proposition 10: If the corresponding curves of the above proposition are long periodic extremals, then they intersect after a half-period $T/2$ and, hence, the associated point belongs to the separating locus.

Proof: For long periodic extremals, one can use the property that the system and the cost are reflectionally symmetric with respect to the equator. Hence, both curves starting from $\dot{\phi}(0)$ and $-\dot{\phi}(0)$ intersect on the antipodal parallel $\pi-\phi(0)$ at the time $T/2$ and with the same cost. It is also true for the θ and r components. □

2. The general case

In the general case, the extremal curves are reflectionally symmetric with respect to meridian planes. Fixing $q(0)=(\phi(0),\theta(0),r(0))$, $(p_\phi(0),p_r(0))$ and considering the two extremal curves with p_θ and $-p_\theta$, one deduces that they are symmetric with respect to the reflexion $(\phi,\theta)\mapsto(\phi,-\theta)$. Hence we have the following.

Proposition 11: If we consider the two extremal curves starting from $q(0)$, $(p_\phi(0),p_r(0),\pm p_\theta)$, then they intersect at the same point and with the same cost on the opposite half meridian and the corresponding point belongs to the separating locus.

D. The geometric properties of the variational equation and estimation of conjugate points

A crucial step in the optimality problem is to analyze the variational equation to estimate the position of conjugate points.[2] It is the object of this section.

1. Preliminaries

Consider a smooth vector field X on a manifold M, $\{\exp tX\}$ denotes the local one parameter group defined by X, $q(t)=\exp[tX(q_0)]$ being the solution starting at $t=0$ from q_0. Fixing such a reference solution defined on $[0,T]$, the linear equation $\delta\dot{q}(t)=\partial X/\partial q(q(t))\delta q(t)$ is called the *variational equation* along $q(t)$ and the linear vector field is denoted by $d\vec{X}$. If $\vec{H}$ is an Hamiltonian vector field on T^*M, and $z(t)=(q(t),p(t))$ a reference curve, then the variational equation defines a linear Hamiltonian vector field. If $\vec{H}$ is associated with an optimal control problem, it is called *Jacobi equation* and the corresponding nonzero solutions $J(t)$ are called Jacobi fields.

We first recall a standard result from differential calculus.

Lemma 1: We have the following.

- *Let $\alpha(s)$, $s\in[0,1]$ be a smooth curve on M such that $\alpha(0)=q_0$, $\dot{\alpha}(s)=v$. Then the derivative of the curve $\beta(s)=\exp tX(\alpha(s))$ at $s=0$ is the solution at time t of the variational equation $\delta\dot{q}=d\vec{X}(q(t))\cdot\delta q$ with the initial condition $\delta q(0)=v$.*
- $d(\exp[tX])=\exp(td\vec{X})$.

2. The integrable case

Clearly in the Hamiltonian case, if the Hamiltonian vector field is Liouville integrable, then the variational equation is integrable [since $d\exp[t\vec{H}]=\exp(td\vec{H})$]. More precisely, from Ziglin's lemma, each first integral F of the motion allows one to construct a first integral F_0 along the reference solution.[7] To make the construction explicit in our case, we proceed as follows. We split the coordinates (q,p) into (q_1,p_1), where $q_1=\phi$, $p_1=p_\phi$ and (q_2,p_2), where $q_2=(r,\theta)$, $p_2=(p_r,p_\theta)$ and the normal Hamiltonian decomposes into

$$H_n(q_1,q_2,p_1,p_2)=p_1a(q_1)+\frac{1}{2}p_1^2b(q_1)+c(q_1,p_2).$$

By construction, one has the following.

Lemma 2: Since q_2 is cyclic, then δq_2 is cyclic for the variational equation and δp_2 is a first integral.

Hence, to integrate the equations, it remains to consider the reduced system

$$\dot{q}_1 = a(q_1) + p_1 b(q_1),$$

$$\dot{p}_1 = -\left[p_1 a'(q_1) + \frac{1}{2} p_1^2 b'(q_1) + c'(q_1, p_2) \right].$$

where $'$ denotes the derivative with respect to q_1. The reduced variational equation is given by

$$\delta\dot{q}_1 = a'(q_1)\,\delta q_1 + b(q_1)\,\delta p_1 + p_1 b'(q_1)\,\delta q_1,$$

$$\delta\dot{p}_1 = -\left[p_1 a''(q_1)\,\delta q_1 + \frac{1}{2} p_1^2 b''(q_1)\,\delta q_1 + c''(q_1, p_2)\,\delta q_1 + a'(q_1)\,\delta p_1 + p_1 b'(q_1)\,\delta p_1 + d(q_1, p_2)\,\delta p_2 \right].$$

Lemma 3: The trajectory $(\dot{q}_1, \dot{p}_1)$ is a solution of the variational equation in which $\delta p_2 = 0$ and the variational equation can be integrated by quadratures.

Proof: The first assertion is a well-known result due to Poincaré and can be easily proven by direct computation. For the second assertion, we observe that the reduced variational equation can be written in the form

$$\delta\ddot{q}_1 + b(t)\,\delta\dot{q}_1 + c(t)\,\delta q_1 = d(t)\,\delta p_2,$$

and since $\psi(t) = \dot{q}_1(t)$ is solution of the right member, if we set $\delta q_1 = \psi(t)x(t)$, then x, is solution of an equation of the form

$$e(t)\ddot{x} + f(t)\dot{x} = d(t)\,\delta p_2,$$

which can be integrated with two quadratures. This proves the second assertion. □

Observe also that the previous lemma is a consequence of the following geometric result.[33]

Proposition 12: If a Lagrangian set of solutions of a linear Hamiltonian equation $\dot{x} = A(t)x$ is known, then a complete set of $2n$-linearly independent solutions can be found by quadratures.

In our cases, such a Lagrangian set can be constructed by taking the tangent space of the train of Lagrangian manifolds $L_t = \exp tH_n(T^*_{q(0)}M)$.

3. Computation of the conjugate locus for short periodic orbits in the meridian case

Here we will study the conjugate locus of small periodic orbits in meridian planes. According to the previous analysis of the phase portraits, these orbits occur if $-\delta^2 a^2/2 < \bar{h} < \delta p_r < 0$ or $-\delta^2 a^2/2 < \bar{h} < 0 < \delta p_r$. Consider an orbits starting at $\phi(0) = \phi_0$ and $r(0) = r_0$. Denote $x_0 = \sin^2 \phi$,

$$M = \sqrt{\delta^2 (1 - x_1) x_2}, \quad k^2 = \frac{x_2 - x_1}{x_2 (1 - x_1)}, \quad z_0^2 = \frac{x_2 (x_0 - x_1)}{x_0 (x_2 - x_1)},$$

where x_1 and x_2 are the roots of the quadratic equation $\bar{h} - W(x) = 0$, more precisely,

$$x_{1,2} = a \pm \sqrt{a^2 + \frac{2\bar{h}}{\delta^2}}.$$

For the values of parameters δp_r and $\bar{h}$ corresponding to the short periodic orbits, we have

$$0 < x_1 \leqslant x_0 \leqslant x_2 < 1,$$

and $k \in]0, 1[$.

The next formulas provide an explicit parametrization for small orbits,

$$x(t) = \frac{x_1 x_2}{x_2 - (x_2 - x_1)\mathrm{sn}(Mt + \psi_0, k)^2},$$

$$r(t) - r_0 = \frac{\delta x_1}{M}\left(\Pi\left(\frac{x_2 - x_1}{x_2}, \mathrm{am}(Mt + \psi_0, k), k\right) - \Pi\left(\frac{x_2 - x_1}{x_2}, \mathrm{am}(\psi_0, k), k\right)\right) - \gamma_+ t,$$

where $\psi_0 = \mathrm{sn}^{-1}(z_0, k)$.

Consider the exponential mapping associated with our problem,

$$\exp_{(\phi_0, r_0), t}: (p_\phi(0), p_r) \mapsto (\phi(t), r(t)).$$

The time t_* is conjugate to $t_0 = 0$ if the differential of $\exp_{(\phi_0, r_0), t}$ is degenerate at $t = t_*$. The extremals of the Hamiltonian system associated with our problem are parametrized by the initial values of the adjoint vector $(p_\phi(0), p_r)$. In order to simplify the further calculation of the differential, it is worth to make a change of variables in the phase space.

Proposition 13: If $\phi(0) \neq \arcsin \sqrt{x_i}$, $i = 1, 2$, *then the map*

$$\Phi: (p_\phi(0), p_r) \mapsto (x_1, k^2)$$

is nondegenerate.

Proof: We can write Φ as a composition map $\Phi = \Phi_3 \circ \Phi_2 \circ \Phi_1$, where

$$(p_\phi(0), p_r) \overset{\Phi_1}{\to} (\bar{h}, a) \overset{\Phi_2}{\to} (x_1, x_2) \overset{\Phi_3}{\to} (x_1, k^2).$$

Then

$$D_{(p_\phi(0), p_r)}\Phi_1 = \begin{pmatrix} \dfrac{\partial \bar{h}}{\partial p_\phi(0)} & \dfrac{\partial \bar{h}}{\partial p_r} \\ \dfrac{\partial a}{\partial p_\phi(0)} & \dfrac{\partial a}{\partial p_r} \end{pmatrix} = \begin{pmatrix} \delta \sin \phi_0 \cos \phi_0 + p_\phi(0) & \dfrac{\partial W}{\partial p_r} \\ 0 & -\dfrac{1}{\delta} \end{pmatrix}.$$

Thus, $\det D_{(p_\phi(0), p_r)}\Phi_1 = 0$ if and only if $\delta \sin \phi_0 \cos \phi_0 + p_\phi(0) = \dot{\phi}(0) = 0$, which occurs at the limit points $\phi_0 = \arcsin \sqrt{x_i}$, $i = 1, 2$, of the orbit. Further,

$$D_{(\bar{h}, a)}\Phi_2 = \begin{pmatrix} \dfrac{\partial x_1}{\partial \bar{h}} & \dfrac{\partial x_1}{\partial a} \\ \dfrac{\partial x_2}{\partial \bar{h}} & \dfrac{\partial x_2}{\partial a} \end{pmatrix} = \begin{pmatrix} -\dfrac{1}{\delta^2 \sqrt{a^2 + \dfrac{2\bar{h}}{\delta^2}}} & 1 - \dfrac{a}{\sqrt{a^2 + \dfrac{2\bar{h}}{\delta^2}}} \\ \dfrac{1}{\delta^2 \sqrt{a^2 + \dfrac{2\bar{h}}{\delta^2}}} & 1 + \dfrac{a}{\sqrt{a^2 + \dfrac{2\bar{h}}{\delta^2}}} \end{pmatrix},$$

hence $\det D_{(\bar{h}, a)}\Phi_2 = -2/\delta^2 \sqrt{a^2 + 2\bar{h}/\delta^2} \neq 0$. Finally, if we denote $m = k^2$, then

$$\det D_{(\bar{x}_1, x)}\Phi_3 = \det \begin{pmatrix} 1 & 0 \\ \dfrac{\partial m}{\partial \bar{x}_1} & \dfrac{\partial m}{\partial x_2} \end{pmatrix} = \frac{\partial m}{\partial x_2} = \frac{x_1}{x_2} \neq 0$$

since $x_1 > 0$.

The statement of the proposition follows now from the chain rule for composition maps. □

The exponential mapping can be written as a composition map of the form

$$\exp_{(\phi_0,r_0),t} = G \circ \Phi,$$

where

$$\Phi\colon (p_\phi(0), p_r) \mapsto (x_1, m), \quad G\colon (x_1, m) \mapsto (\phi(t), r(t)).$$

According to Proposition 13, the map Φ is nondegenerate if $\phi_0 \neq \arcsin\sqrt{x_{1,2}}$. Hereafter, we assume that this condition is verified. Thus, critical points of the exponential mapping correspond to the critical points of G. Recall that $x(t) = \sin 2\phi(t)$, hence,

$$D_{(x_1,m)}G = \frac{\partial \phi}{\partial x} D_{(x_1,m)}G_1, \quad G_1\colon (x_1, m) \mapsto (x(t), r(t)).$$

According to the parametrization of the solution,

$$x(t) = \bar{x}(z(t; x_1, m); x_1, m) = \frac{x_1}{1 - m(1 - x_1)z(t)^2},$$

where $z(t) = \mathrm{sn}(Mt + \psi_0, k)$ with

$$M = \left(\frac{\delta^2 x_1 (1 - x_1)}{1 - m(1 - x_1)} \right)^{1/2}, \quad \mathrm{sn}(\psi_0, k) = z(0).$$

Thus,

$$\Delta = D_{(x_1,m)}G_1 = \begin{pmatrix} \dfrac{\partial \bar{x}}{\partial z}\dfrac{\partial z(t)}{\partial x_1} + \dfrac{\partial \bar{x}}{\partial x_1} & \dfrac{\partial \bar{x}}{\partial z}\dfrac{\partial z(t)}{\partial m} + \dfrac{\partial \bar{x}}{\partial m} \\ \dfrac{\partial r(t)}{\partial x_1} & \dfrac{\partial r(t)}{\partial m} \end{pmatrix}.$$

In order to shorter the notations, below we will write sn for $\mathrm{sn}(Mt + \psi_0, k)$, and similarly for other elliptic functions. The direct calculation yields

$$\frac{\partial \bar{x}}{\partial x_1} = \frac{\mathrm{dn}^2}{(1 - m(1 - x_1)\mathrm{sn}^2)^2}, \quad \frac{\partial \bar{x}}{\partial m} = \frac{x_1(1 - x_1)\mathrm{sn}^2}{(1 - m(1 - x_1)\mathrm{sn}^2)^2},$$

$$\frac{\partial \bar{x}}{\partial z} = \frac{2m(1 - x_1)x_1\,\mathrm{sn}}{1 - m(1 - x_1)\mathrm{sn}^2}.$$

Hence,

$$\Delta = \frac{\Delta_1}{(1 - m(1 - x_1)\mathrm{sn}^2)^2},$$

where

$$\Delta_1 = \begin{pmatrix} 2mx_1(1 - x_1)\mathrm{sn}\dfrac{\partial z(t)}{\partial x_1} + \mathrm{dn}^2 & 2mx_1(1 - x_1)\mathrm{sn}\dfrac{\partial z(t)}{\partial m} + x_1(1 - x_1)\mathrm{sn}^2 \\ \dfrac{\partial r(t)}{\partial x_1} & \dfrac{\partial r(t)}{\partial m} \end{pmatrix}.$$

For convenience, we denote $T = Mt$,

$$\mathrm{sn}_0 = z(0), \quad \mathrm{cn}_0 = \mathrm{cn}(\psi_0, k), \quad \mathrm{dn}_0 = \mathrm{dn}(\psi_0, k).$$

We finally find the following expression:

$$\Delta_1 = -\frac{M\,\mathrm{cn}\,\mathrm{sn}\,\mathrm{dn}}{8}\left[T^2 - \frac{1}{1-m}\left(E_T - \frac{\mathrm{dn}\,\mathrm{sn}}{\mathrm{cn}} + \frac{\mathrm{dn}_0\,\mathrm{sn}_0}{\mathrm{cn}_0}\right)\left(E_T + \frac{\mathrm{dn}\,\mathrm{cn}}{\mathrm{sn}} - \frac{\mathrm{dn}_0\,\mathrm{cn}_0}{\mathrm{sn}_0}\right)\right],$$

where

$$E_T = \int_{\psi_0}^{T+\psi_0} \mathrm{dn}^2(\xi,k)d\xi.$$

Conjugate times t_* are solutions of the equation

$$\Delta_1(t_*) = -\frac{M\,\mathrm{cn}\,\mathrm{sn}\,\mathrm{dn}}{8}\,\Delta_2|_{t=t_*} = 0. \tag{8}$$

It is not difficult to note that solutions of (8) are actually zeros of $\Delta_2(t_*)$ term. A more symmetric form for it can be obtained using the integral formula for E_T and the standard relations among elliptic functions. Indeed,

$$\begin{aligned}
&\frac{1}{1-m}\left(E_T - \frac{\mathrm{dn}\,\mathrm{sn}}{\mathrm{cn}} + \frac{\mathrm{dn}_0\,\mathrm{sn}_0}{\mathrm{cn}_0}\right)\left(E_T + \frac{\mathrm{dn}\,\mathrm{cn}}{\mathrm{sn}} - \frac{\mathrm{dn}_0\,\mathrm{cn}_0}{\mathrm{sn}_0}\right)\\
&\quad= \frac{1}{1-m}\int_{\psi_0}^{T+\psi_0} 1 - \frac{\mathrm{dn}^2(\xi,k)}{\mathrm{cn}^2(\xi,k)}d\xi \cdot \int_{\psi_0}^{T+\psi_0} 1 - \frac{1}{\mathrm{sn}^2(\xi,k)}d\xi\\
&\quad= \left(T + \int_{\psi_0}^{T+\psi_0} \frac{1}{\mathrm{cn}^2(\xi,k)}d\xi\right)\left(T - \int_{\psi_0}^{T+\psi_0} \frac{1}{\mathrm{sn}^2(\xi,k)}d\xi\right).
\end{aligned}$$

By setting

$$I_1^T = \int_{\psi_0}^{T+\psi_0} \frac{1}{\mathrm{cn}^2(\xi,k)}d\xi, \quad I_2^T = \int_{\psi_0}^{T+\psi_0} \frac{1}{\mathrm{sn}^2(\xi,k)}d\xi,$$

we finally get

$$\Delta_2 = T(I_2^T - I_1^T) + I_1^T I_2^T.$$

We remark that both integrals I_1^T and I_2^T are positive monotone increasing functions of T, and they both diverge as $T \to nK(k) - \psi_0$ for $n \in \mathbb{N}$. The numerical tests suggest that the first conjugate point occur after one period of ϕ-variable $(2K(k)/M)$.

We present in Fig. 3 the behavior near the origin of a family of orbits, starting at $r_0 = -1$ and $x_0 = 0.35$ for $\delta = 3$, $p_r = 0.01$, and $\gamma_+ = 6.1$, calculated up to the first conjugate point (marked by "$*$"). The polar coordinates of the initial point in this example are $\rho_0 = e^{-1}$ and $\phi_0 \cong 0.633\,052$. The short periodic solutions for ϕ exist for $\bar{h} \in]-1.11, 0[$. The solutions on the figure correspond to $\bar{h} = -1$, -0.9, -0.8, -0.7, -0.6, -0.5, -0.4, and -0.2. The sign "|" marks the end of the first period of $\phi(t)$. Illustrated solutions asymptotically tend to the origin, but loose the optimality before, just after the end of the first period.

E. The value function and Hamilton–Jacobi–Bellman equation

Definition 4: Fixing the initial point to q_0, the value function $S(T,q)$ is the optimal cost to steer q_0 to q in time T. Computing the value function in a conic neighborhood of a reference extremal curve is called a microlocal solution.

1. The abnormal case

This analysis is mainly based on the work,[12] restricting to the simple 2D-situation (see also Refs. 40 and 41).

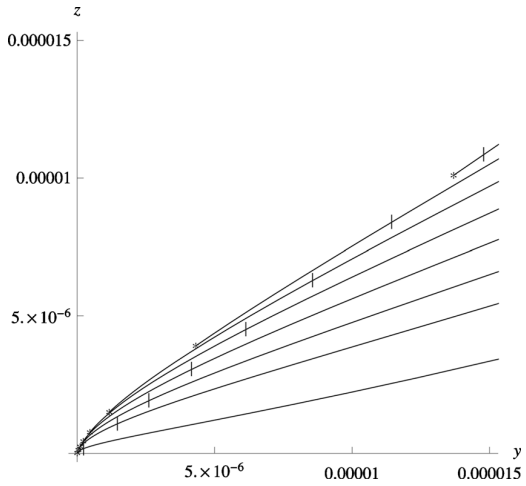

FIG. 3. Behavior near the origin of a family of orbits (see the text).

Preliminaries. According to our previous analysis, one can restrict our study to the 2D-system in the meridian planes, where the control u is restricted to the real field. If $\gamma_+ - \Gamma \neq 0$, the two abnormal lines are the z-axis of revolution and an horizontal line. Except at collinear point where $\det(F_0, F_1) = 0$ and at the intersection I of the two lines, one can construct the following normal form along a reference abnormal curve $q(\cdot)$. The vector field F_1 is identified to $\partial/\partial y$, while the abnormal trajectory is identified to $q(\cdot): t \mapsto (t, 0)$. This leads to the model

$$\dot{x} = 1 + a(x)y^2 + o(y^2),$$

$$\dot{y} = b(x) + O(y) + u,$$

where y is small in a C^0-neighborhood of the reference abnormal trajectory. The abnormal control along the reference trajectory is $u_a = -b(x)$ and we choose a control bound $|u| \leqslant M$ with M large enough such that u_a is admissible and not saturating, that is, $|u_a| < M$. From the model, we immediately observe that in a C^0-neighborhood of the reference abnormal trajectory, in the limit case $M = +\infty$, the reference abnormal control is

- time-minimal if $a(x) < 0$, which corresponds to the hyperbolic situation, and
- time-maximal if $a(x) > 0$, which corresponds to the elliptic situation.

Consider now the time minimal control problem for the system, with the control bound $|u| \leqslant M$. One can easily construct the accessibility set $A(q_0, T)$ along a reference abnormal direction, where q_0 is identified to 0. In the hyperbolic case, from the classification of the extremal curves near a point such that $H_1 = \{H_1, H_0\} = 0$, each time-minimal curve starting from q_0 is an abnormal arc, followed by a bang arc $|u| = M$ and the same is true for the time-maximizing problem in the elliptic case. The same holds also in the limit case $M \to +\infty$ where the boundary tends to the vertical line.[10] Hence, according to the maximum principle, the boundary of the accessibility set $A(q_0, T)$ is near point A, extremity of the abnormal direction, a C^1 curve which is formed by taking an abnormal arc, followed by a bang arc $|u| = M$. The same holds also in the limit case $M \mapsto +\infty$, when the boundary tends to the vertical line. In particular, we deduce the following proposition.

Proposition 14: Let A be the extremity point at time T of the abnormal line starting from 0. Then the abnormal control is the only control steering 0 to A in time T provided the corresponding trajectory remains in a tube around the x-axis. In other words, the abnormal line is C^0-isolated and, hence, is C^0-optimal for the energy minimization problem.

The next step is to compute the value function in the abnormal direction. The model is

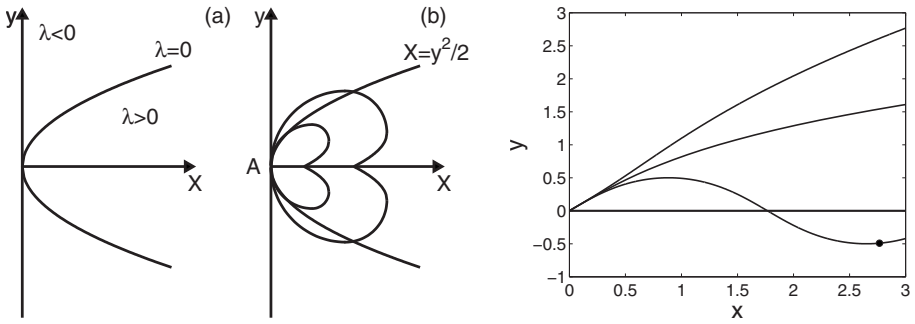

FIG. 4. Foliation of $A(0,1)$ (a) and level sets of the value function (b). (Bottom panel) Conjugate point analysis. Numerical values are taken to be $\lambda=-4,0,4$, $p_y(0)=1$ from top to bottom.

$$\dot{x} = 1 + a(x)y^2,$$

$$\dot{y} = b(x) + u, \quad \min \int_0^{t_f} u^2 dt,$$

where $x \sim t$. Let $X=x-t$, one gets

$$\dot{X} = a(t)y^2, \quad \dot{y} = b(t) + u.$$

One can assume $a>0$ and setting $Y=a^{1/2}y$, we obtain

$$\dot{X} = Y^2, \quad \dot{Y} = \sqrt{a}y + a^{1/2}\dot{y} \sim a^{1/2}(b+u).$$

A simplification occurs when the reference abnormal control is zero, which is an important situation encountered in our application. To summarize, this leads to analyze the simplified problem,

$$\dot{x} = 1 + y^2, \quad \dot{y} = u, \quad \min \int_0^1 u^2 dt,$$

which is the working example analyzed in Ref. 40. In this example, the normal extremals are defined by the Hamiltonian

$$H_n = p_x(1+y^2) + \frac{1}{2}p_y^2.$$

Setting $p_x=\lambda/2$, the normal extremals are solutions of the pendulum equation,

$$\ddot{y} + \lambda y = 0, \quad \lambda = 2p_x.$$

One gets three types of normal extremals which are necessary to compute the value function, starting from 0.

- $\lambda=0$: $y(t)=At+B$. Starting from 0, one gets $y(t)=At$ and $x(t)=t+At^2/2=1+y^2/2$ if $t_f=1$, which defines a separating parabola $X=y^2/2$.
- $\lambda<0$: one has $y(t)=C\sinh(\sqrt{|\lambda|}t)$.
- $\lambda>0$: one has $y(t)=C\sin(\sqrt{|\lambda|}t)$.

In Fig. 4, we have represented the level sets of the value function. *The value function is not continuous in A*, the cost being zero along the abnormal direction and the level sets are ramifying at A. We observe two phenomena related to the abnormal direction. First of all, the value function near A is constructed using hyperbolic trajectories ($\lambda<0$) and computing this leads to $S(x,y)$

$\simeq y^4/4X$. Point A is obtained on a given level set r for $\lambda \to -\infty$. This is the *phenomenon of nonproperness of the exponential mapping* restricted to the optimal extremal curves. A second property is observed: the level sets are not smooth along the abnormal direction because of the existence of cut points. This is related to oscillations of normal extremals in the elliptic case where $\lambda > 0$. An additional property is the existence of conjugate points represented in Fig. 4 (bottom) and which occur after the cut point.

Stability analysis. This working example allows one to understand the level sets of the value function near point A extremity of the abnormal direction and gives the singularity analysis for the true system of the level sets for $r > 0$ small when the abnormal direction is associated with a zero control. We obtain two sectors: the one that corresponds to the hyperbolic trajectories, where the level sets are ramifying, and the one corresponding to the elliptic trajectories, where the cut points accumulate. The model is not generic since the extremal curves are reflectionally symmetric with respect to the abnormal direction. In the general case, b is not zero and the normal Hamiltonian system is not integrable. Nevertheless, since cut points are not conjugate points, this situation is stable and allows one to evaluate the cut locus near A. For the hyperbolic sector, the exponential mapping is not proper and this is a stable property. However, asymptotic expressions of the level sets cannot be computed. Still we conjecture that due to the 2D-situation, the ramification phenomenon is stable.

Computations for the quantum system. From the computation of the Poisson brackets, one gets the following proposition.

Proposition 15: The abnormal curves for $\delta = \gamma_+ - \Gamma \neq 0$ *will form the two lines*.

(1) *The z-axis of revolution* $y = 0$, *the corresponding abnormal control being given by* $u_a = 0$.
(2) *The abnormal line* $z = \gamma_-/2(\gamma_+ - \Gamma)$, *the abnormal control being given by* $u_a = \gamma_-(\gamma_+ - 2\Gamma)/2y(\gamma_+ - \Gamma)$, *which is blowing up for* $y = 0$ *if* $\gamma_-(\gamma_+ - 2\Gamma) \neq 0$. *In particular, the abnormal control for* $\gamma_- = 0$ *is zero*.

To apply the previous singularity resolution, one must exclude the case where the singular line is meeting the collinear set $\det(F_0, F_1) = 0$. For the vertical line, it corresponds to (0,0) and $(0, \gamma_-/\gamma_+)$. For the horizontal line, if $\gamma_- = 0$, it corresponds to (0,0), if $\gamma_- \neq 0$ and $\gamma_+ - 2\Gamma \neq 0$ this intersection is empty and if $\gamma_+ = 2\Gamma$, it reduces to $y = 0$. Also one must exclude I, the intersection point of the two singular lines. In particular, as a conclusion of our analysis we have the following proposition.

Proposition 16: Assume that $\delta = \gamma_+ - \Gamma \neq 0$. *Then for the energy minimization problem with fixed transfer time and initial condition on the z-axis, the abnormal trajectory along the z-axis is optimal and the singularity resolution along the abnormal line is valid up to meeting the collinear set* ($z = 0$ *or* $z = \gamma_-/\gamma_+$) *or the intersection point I of the abnormal lines. The same holds if* $\gamma_- = 0$ *for the y-axis up to the origin. In the general case* $\gamma_- \neq 0$, *the optimality status holds up to meeting the z-axis of revolution*.

In fine, an important consequence of our analysis is the following proposition.

Proposition 17: For the energy minimization problem, every optimal curve is smooth.

Proof: From Proposition 16, every optimal curve is extremal. Using the previous analysis, one cannot connect abnormal and normal extremals. This proves the assertion. □

2. The Hamilton–Jacobi–Bellman theory in the normal case

Before going further in the analysis, we shall present results about Hamilton–Jacobi–Bellman theory adapted to our study. This crucial presentation is mainly due to Ref. 27. It concerns the relation between Hamilton–Jacobi equations and Lagrangian manifolds.

Preliminaries. We consider a general smooth control problem on a manifold: $\dot{q} = F(q, u)$, while the cost function to be minimized is $\varphi(u) = \int_0^T c(q, u)dt$ and the control domain is U. Let $z = (q, p) \in T^*M$ and introduce the pseudo-Hamiltonian,

$$\tilde{H}_{p_0}(z,u) = \langle p, F(q,u)\rangle - p_0 c(q,u),$$

where $p_0 \geqslant 0$. The normal case corresponds to $p_0 > 0$ and it can be normalized to +1. The following result is standard but crucial.

Proposition 18: Let

$$(\bar{z},\bar{u}):\bar{J} = [\bar{\alpha},\bar{\beta}] \mapsto T^*M \times U$$

be a normal smooth reference extremal curve. Assume that there exists an open neighborhood W of $\bar{q}(\bar{J})$ *and two smooth mappings* $S: W \to \mathbb{R}$, $\hat{u}: W \to U$ *such that*

(i) $\bar{p}(t) = dS(\bar{q}(t))$ *for each* $t \in \bar{J}$, $\bar{u}(t) = \hat{u}(\bar{q}(t)) \in U$ *for each* $t \in \bar{J}$.

(ii) $\forall (q,u) \in W \times U: \bar{H}_1(dS(q),u) \leqslant \bar{H}_1(dS(q),\hat{u}(q))$.

(iii) *There exists a constant h such that* $\bar{H}_1(dS(q),\hat{u}(q)) = h$.

Then the reference extremal is optimal with respect to all smooth curves solutions, contained in the neighborhood W, with the same extremities, and we have two cases:

(a) $h = 0$: *transfer time not fixed* and

(b) $h \neq 0$: *transfer time fixed.*

Proof: Let q be a smooth curve on $J = [\alpha,\beta]$, with the same extremities

$$\bar{q}(\bar{\alpha}) = q(\alpha), \quad \bar{q}(\bar{\beta}) = q(\beta)$$

and we denote the cost by $\varphi(q,u) = \int_\alpha^\beta c(q(t),u(t))dt$. One has

$$c(q(t),u(t)) = \langle F(q(t),u(t)), dS(q(t))\rangle - \bar{H}_1(dS(q(t),u(t))),$$

which can be written as

$$c(q(t),u(t)) = dS(q(t))\dot{q}(t) - \bar{H}_1(dS(q(t),u(t))) = \frac{d}{dt}S(q(t)) - \bar{H}_1(dS(q(t),u(t))).$$

Therefore,

$$\varphi(q,u) = S(q(\beta)) - S(q(\alpha)) - \int_\alpha^\beta \bar{H}_1(dS(q(t),u(t)))dt.$$

Similarly,

$$\varphi(\bar{q},\bar{u}) = S(\bar{q}(\bar{\beta})) - S(\bar{q}(\bar{\alpha})) - \int_{\bar{\alpha}}^{\bar{\beta}} \bar{H}_1(dS(\bar{q}(t),\bar{u}(t)))dt.$$

Hence,

$$\varphi(q,u) - \varphi(\bar{q},\bar{u}) = \int_{\bar{\alpha}}^{\bar{\beta}} \bar{H}_1(dS(\bar{q}(t),\bar{u}(t)))dt - \int_\alpha^\beta \bar{H}_1(dS(q(t),u(t)))dt,$$

and from cases (ii) and (iii)

$$\bar{H}_1(dS(q(t),u(t))) \leqslant h, \quad \bar{H}_1(dS(\bar{q}(t),\bar{u}(t))) = h.$$

One deduces that

$$\varphi(q,u) - \varphi(\bar{q},\bar{u}) \geqslant h[(\bar{\beta} - \bar{\alpha}) - (\beta - \alpha)].$$

Hence, we have if $h=0$, $\varphi(q,u) \geqslant \varphi(\bar{q},\bar{u})$; if $h \neq 0$ and $\beta-\alpha=\bar{\beta}-\bar{\alpha}$, again one has $\varphi(q,u) \geqslant \varphi(\bar{q},\bar{u})$. □

Construction of S and $\hat{u}$. The next step consists in constructing S and $\hat{u}$. It is based on the standard theory of *extremal fields* in calculus of variations, extended to optimal control. It is presented for the energy minimization problem, but the construction is general.

We select a reference extremal $\bar{z}(t)=(\bar{q}(t),\bar{p}(t)), t \in [0,T]$ solution of the Hamiltonian vector field $\vec{H}_n$, with $H_n=H_0+\frac{1}{2}(H_1^2+H_2^2)$, corresponding to the normal case. One assumes that the reference extremal curve $\bar{q}(t)$ is one-to-one on $[0,T]$. Let $L_0=T^*_{\bar{q}(0)}M$ be the fiber and from standard symplectic geometry the set $L_t=\exp t\vec{H}_n(L_0)$ will form a *train of Lagrangian manifolds*, along the reference extremal curve.

If h is the level set $H_n=h$ of the reference extremal $\bar{z}(t)$, the reference curve can be embedded in the *central field:* $\bar{W}=\exp[t\vec{H}_n(p(0))]$, restricting to the level set $H_n=h$ and $p(0)$ close enough to $\bar{p}(0)$. This field is $\Pi(\cup_{t\geqslant 0}L_t \cap (H_n=h))$. This embedding is locally one-to-one provided the exponential mapping $\exp_{q(0)}$ restricted to the level set $H_n=h$ is one-to-one along the reference extremal. This is clearly equivalent to the *nonexistence of conjugate point condition:* $\operatorname{rank}(\delta q(t),\dot{\bar{q}}(t)) = \dim M$, where $\delta q(t)$ is the Π-projection of the fields $\delta z(t)$ restricting the variational equation $\delta\dot{z}(t)=d\vec{H}_n(\bar{z}(t))\,\delta z(t)$ to the level set $H=h$ and forming the tangent space to $L_t \cap (H_n=h)$ along $\bar{z}(t)$.

In this case, $L=\cup_{t\geqslant 0}L_t \cap (H_n=h)$ is again a Lagrangian manifold, union of isotopic manifolds of codimension 1, along the reference extremal curve $\bar{z}(t)$ and, moreover, the standard projection Π from L to M is locally one-to-one. Therefore, L is a graph $\left(q,p=\frac{\partial S}{\partial q}\right)$ whose generating mapping S is the mapping to construct. We observe that the construction of S amounts to solve the Hamilton–Jacobi–Bellman equation

$$H_n\left(q,\frac{\partial S}{\partial q}\right) = h,$$

which is a standard reduction of the more general equation,

$$\frac{\partial \bar{S}}{\partial t} + H_n\left(q,\frac{\partial \bar{S}}{\partial q}\right) = 0,$$

where $\bar{S}(t,q)$ is the value function, depending on the final condition q and the transfer time t, S and $\bar{S}$ being related by $\bar{S}(t,q)=S-ht$.

This construction can be extended in a maximal simply connected domain W of the reference extremal curve $\bar{q}(t)$. This corresponds to the domain W in Proposition 18.

The integrable case. We consider the situation where $\gamma_-=0$. The following proposition is clear.

Proposition 19: If $\gamma_-=0$, the complete solution of the corresponding Hamilton–Jacobi–Bellman problem can be computed by the separation of variables.

A further step is necessary to determine the value function. Since the extremal solutions in the normal case are given by elliptic functions, to compute the value function, one must solve the shooting equation: $\exp_{q_0}(T,p(0))=q_1$. This amounts to inverse the exponential mapping and to use the inverses of elliptic functions. Concerning the microlocal point of view, we observe that we have two microlocal solutions corresponding to short and long periodic trajectories. The long ones are generalizations of the trajectories in the Grushin case and correspond to optimal curves for reaching points after crossing the equator.

3. The global Hamilton–Jacobi–Bellman equation

The singularity analysis. In order to compute the global optimality synthesis, one must solve the Hamilton–Jacobi–Bellman equation on the whole domain. To simplify the presentation, we

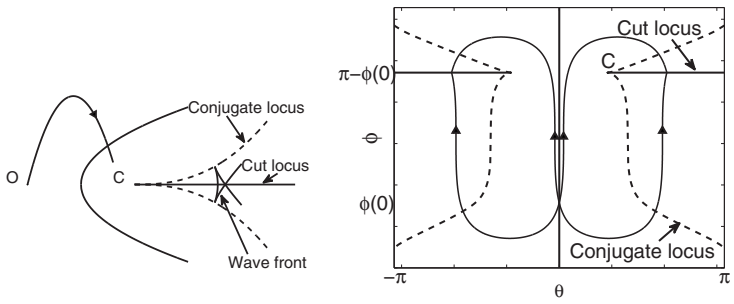

FIG. 5. (Top) Generic microlocal case. (Bottom) The Grushin case.

shall only consider the restricted problem where $\gamma_{-}=0$ and r is not controlled. The final transfer time T is fixed, but has to be taken as a parameter of the problem. For each such fixed T, one can introduce the *sphere of radius* r: $S(q_0,r)$, formed by extremities of optimal curves, with fixed cost r. Thanks to the existence theorem, it can be computed restricting to extremal curves. The sphere is a subset of the *wave front of radius* r, denoted by $W(q_0,r)$, formed by extremities at time T of extremal curves with cost r. By looking at the propagation of spheres and wave fronts, one can construct the optimal synthesis. From classical singularity theory, the singularities of such objects are related to Lagrangian and Legendrian singularity theory. We next recall the generic situation (see Ref. 18 for the details).

According to Thom's point of view, the mathematical model comes from optics. More precisely, we consider a source point O, which generates waves. Assume that at a given time the wave front is exactly a parabola and for further time we assume that it propagates along the normals, according to the rules of propagation of light. One must compute starting from a parabola the sphere and wave front for the flat metric $g=dx^2+dy^2$, while the normal propagation rule corresponds exactly to the transversality condition of the maximum principle. The complete computation is presented in Fig. 5 (top). The conjugate locus has a cusp at C and corresponds to the generic singularity associated with Lagrangian singularity theory, while sections of a swallowtail represent the singularities of the wave front.[23] It is also the generic singularity coming from Legendrian singularity theory. The cut locus is formed by the set of points where two optimal curves intersect, the limit case being point C, which is a conjugate point representing also the distance from the source to the cut locus. In other words, the cut locus is the union of the separating locus with the cusp point C of the conjugate locus.

Further work is necessary[8] to deduce the geometric situation in the Grushin case, for an initial point $q(0)=(\phi(0),\theta(0))$ not a pole nor on the equator. It is represented in Fig. 5 (bottom). The cut locus is a single branch on the antipodal parallel, while the conjugate locus has a standard astroid shape with four cusps. The main property to obtain this global solution is the discrete symmetry group corresponding to reflexions with respect to the equator or the meridians.

Next we present the geometric point of view to construct the solution numerically.

The general case. In the general case, for fixed T one must construct the propagation of the wave front. A dual point of view is to consider for each fixed $H_n=h$ the evolution of the wave front with respect to time. In the Grushin case, both are equivalent and by homogeneity the level set can be fixed to $h=1/2$. If $\phi(0)\neq\pi/2$, we are in the Riemannian case and the exponential mapping is defined on a circle, while if $\phi(0)=\pi/2$, this domain is no more compact since p_θ belongs to the whole $\mathbb{R}$.

In the integrable case, restricting to $p_r=0$, the level set $H_n=h$ takes the following form:

$$(p_\phi+\delta\sin\phi\cos\phi)^2+p_\theta^2\cot^2\phi=2h+\delta^2\sin^2\phi\cos^2\phi.$$

Hence, one must have

$$h \geqslant -\frac{\delta^2}{2}\sin^2\phi(0)\cos^2\phi(0)$$

and setting

$$\varepsilon^2 = 2h + \delta^2\sin\phi(0)\cos^2\phi(0), \quad X = p_\theta\cot\phi(0), \quad Y = p_\phi(0) + \delta\sin\phi(0)\cos\phi(0),$$

the domain of the exponential mapping is for each h, the set $X^2+Y^2=\varepsilon^2$, where again p_θ is bounded except if $\phi(0)=\pi/2$. If $\phi(0)\neq\pi/2$, it shrinks into a point if $h=h_0=-\delta^2\sin^2\phi(0)\cos^2\phi(0)/2$, while for $h>h_0$, one gets short and long periodic trajectories as discussed in Sec. II C.

The same construction is valid in dimension 3, in the integrable case where p_r is any constant. The level set $H_n=h$ is again written as

$$(p_r-\delta\cos^2\phi)^2 + (p_\theta\cot\phi)^2 + (p_\phi+\delta\sin\phi\cos\phi)^2 = 2h + \delta^2\sin^2\phi\cos^2\phi + 2p_r\Gamma + p_r^2 + \delta^2\cos^4\phi. \tag{9}$$

A lifting of the problem can be made, taking into account the homogeneity properties of the system. For that, it is sufficient to introduce the extended adjoint vector $\tilde{p}=(p_r,p_\theta,p_\phi,\delta)$ and denoting $\tilde{q}=(r,\theta,\phi,x_\delta)$ the extended state variable, $\tilde{M}=\mathbb{R}^2\times S^2$ being the extended state space and $T^*\tilde{M}$ is endowed with the Liouville symplectic structure: $d\tilde{q}\wedge d\tilde{p}$.

Hence, the equation $H_n=h$ can be written as

$$\frac{1}{2}\sum_{i=1}^{3}\langle\tilde{p},G_i(\tilde{q})\rangle^2 = \Delta, \tag{10}$$

where according to (9), the vector fields are defined by

$$G_1 = \frac{\partial}{\partial r} - \frac{\partial}{\partial x_\delta}\cos^2\phi,$$

$$G_2 = \cot\phi\frac{\partial}{\partial\theta},$$

$$G_3 = \frac{\partial}{\partial\phi} + \sin\phi\cos\phi\frac{\partial}{\partial x_\delta},$$

while Δ corresponds to the right member.

One further lifting is needed since the Grushin metric $g=d\phi^2+\tan^2\phi d\theta^2$ is singular at the equator. To make the construction, we observe that near the equator, the Grushin metric is represented by the quasihomogeneous local model $g=d\bar{r}^2+\bar{r}^{-2}d\theta^2$, with corresponding Hamiltonian $H=\frac{1}{2}(p_{\bar{r}}^2+\bar{r}^2p_\theta^2)$. Introducing the auxiliary variable ψ, such an Hamiltonian corresponds to the restriction of the Hamiltonian,

$$H = \frac{1}{2}\left(p_{\bar{r}}^2 + \left(\frac{p_\psi}{\bar{r}} - \bar{r}p_\theta\right)^2\right)$$

to the space $p_\psi=0$. An easy computation shows that such an Hamiltonian is the standard Hamiltonian,

$$H = \frac{1}{2}[(p_x^2 + p_y^2) - 2p_z(xp_y - yp_z) + (x^2 + y^2)p_z^2],$$

written using the cylindric coordinates. This Hamiltonian describes the evolution of extremal trajectories in sub-Riemannian (SR)-geometry in the Heisenberg case.[10]

If we apply this lifting process to (10), it can be written as

$$\frac{1}{2}\sum_{i=1}^{3} \langle \tilde{p}', G_i'(\tilde{q}') \rangle^2 = \Delta,$$

where the vector field G_i' is the lifting of G_i to the extended space $\tilde{q}' = (\bar{r}, \tilde{q})$. Moreover, we observe that one can write

$$\Delta = 2h + 2p_r\Gamma + p_r^2 + o(\delta).$$

Making δ=0 in the right member, we see that the corresponding Hamiltonian solutions are precisely the extremities of the SR-problem

$$\dot{\tilde{q}}' = \sum_{i=1}^{3} u_i G_i'(\tilde{q}'), \quad \min_{u(\cdot)} \int_0^T \sum_{i=1}^{3} u_i^2(t)dt.$$

Hence, for δ small enough, the corresponding SR-problem is an approximation of our problem. This remark is important for two reasons. First of all, SR-geometry is a well developed research area. In particular, it is a geometry where many microlocal situations have been analyzed (see, for instance, the Martinet case in Ref. 10). This is clearly related to the microlocal situations encountered in our analysis.

IV. GEOMETRIC ALGORITHMS AND NUMERICAL SIMULATIONS

A modern and pragmatic treatment of such an optimal control problem needs the development of appropriate geometric algorithms and appropriate codes which are used to make the numerical simulations. Such codes based on the techniques of geometric control theory are an important work mainly developed in a parallel research project in orbital transfer, where low propulsion technique was used. We shall make a short presentation of these codes, prior to the presentation of the numerical results.

A. The COTCOT code

The role of this code is to compute extremals and conjugate points in the case where the Hamiltonian describing the extremal field is smooth. Noting H_n this Hamiltonian and fixing the extremities q_0, q_1 of the problem, the extremals are solutions of

$$\dot{z}(t) = \vec{H}_n(z(t)),$$

and if the boundary conditions are given by q_0 and q_1, one must find the zeros of the *shooting equation*,

$$E:(T, p_0) \mapsto \Pi(\exp T\vec{H}_n(q_0, p_0)) - q_1,$$

where T is the transfer time.

In order to compute the conjugate points, one must compute in parallel the Jacobi fields solutions of the variational equation,

$$\delta\dot{z}(t) = d\vec{H}_n(z(t))\,\delta z(t)$$

along the given extremal.

The aim of the code COTCOT (Conditions of Order Two, COnjugate Times[19]) is to provide the numerical tools:

(1) to integrate the smooth Hamiltonian vector field $\vec{H}_n$,
(2) to solve the associated shooting equation,
(3) to compute the corresponding Jacobi fields along the extremals, and
(4) to evaluate the resulting conjugate points.

The code is written in FORTRAN language, while automatic differentiation is used to generate the Hamiltonian differential equation and the variational one. For the users, the advanced language is MATLAB (see Ref. 9 for a precise description of the COTCOT code with the underlying algorithms: ordinary differential equation (ODE) integrators, Newton method solver). The conjugate point test consists of checking a rank condition, which is based on two methods: evaluating zeros of a determinant or a singular value decomposition.

B. The smooth continuation method

The smooth continuation method is an important numerical approach to solve a system of equations $F(x)=0$, where $F:\mathbb{R}^n\to\mathbb{R}^n$ is a smooth mapping. The principle is to construct an homotopy path $H(x,\lambda)$ such that $H(x,0)=G(x)$ and $H(x,1)=F(x)$, where $G(x)$ is a map having known zeros or where the zeros can be easily computed using a Newton-type algorithm. The zeros are computed along the path with this method and at each step the procedure is implemented with the zeros computed at the previous step (see Ref. 6 for the details). It is a general approach which has to be adapted to optimal control problems: the shooting equation comes from the projection of a symplectic mapping, the Jacobian can be computed using Jacobi fields and one must consider the central extremal field associated with the problem (see Ref. 13 for the geometric concepts). A short description of the method is given below in our case study.

We consider the family of smooth Hamiltonians H_λ, where $\lambda\in\Lambda=(\Gamma,\gamma_+,\gamma_-)$ belongs to the set of dissipative parameters. Assume that one wants to solve the shooting equation, associated with a fixed end-point conditions q_0, q_1 and for a specific value of the parameter λ_1, that is, $E(x)=q_1$ where

$$E{:}x=p(0)\mapsto \exp^{\lambda}_{q_0}(T,p(0))=q_1.$$

The smooth continuation method has to be initialized by choosing a value λ_0 of the parameter for which the solution is known or can be computed numerically. This leads to an initial value x_0 of the adjoint vector $p(0)$.

A simple numerical scheme is to discretized the homotopy path from λ_0 to λ_1 identified to $[0,1]$ as $0=\lambda_0'<\lambda_1'\cdots<\lambda_N'=1$ where the shooting equation is solved iteratively using a Newton-type method: $x_{i+1}=x_i-E'^{-1}(x_i)E(x_i)$.

Clearly we have (see Lemma 1) the following.

Proposition 20: For each λ, the shooting equation is of maximal rank if and only if point q_1 is not conjugate to q_0, for the corresponding H_λ. Moreover, in this case, the solutions of the parametrized shooting equation form a smooth curve which can be parametrized by λ and the derivative E' can be generated by integrating the Jacobi equation.

If the simplest numerical scheme discretizing the homotopy path cannot be used, a refined approach consists of following the smooth path of the zeros solutions by integrating along the path the implicit ODE describing this set. In this case, a unique shooting is necessary to initialize the continuation method. A numerical scheme was recently developed from this algorithm. This will be used to complete the COTCOT code in the numerical simulations below.

The convergence of the continuation methods are related to the following.

(1) From a microlocal point of view, the problem is to control the distance (for the energy cost) to the conjugate locus $C(q_0,\lambda)$.

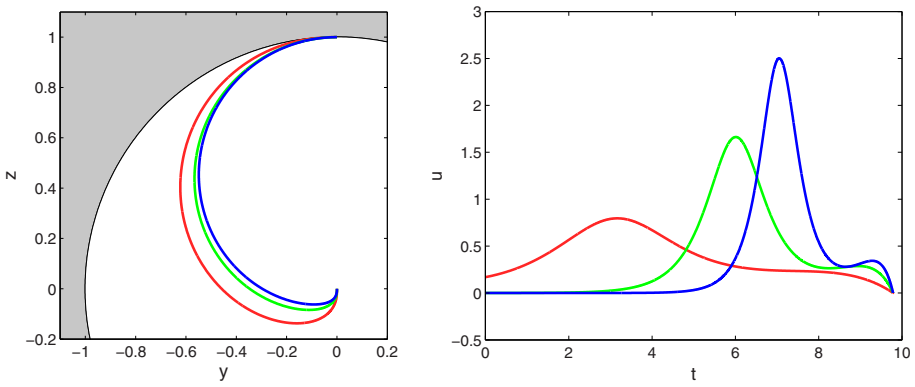

FIG. 6. (Color online) (Top) Plot of the different optimal trajectories (top) and of the corresponding control fields (bottom) for different dissipation parameters. Numerical values are, respectively, taken to be $\delta=\Gamma-\gamma=0.47$, 1.24, and 2.02 for the red (dark gray), green (light gray), and blue (black) trajectories.

(2) From a global point of view, the problem is to control the distance to the cut locus $C_{ut}(q_0,\lambda)$.

We observe that according to our geometric analysis, this amounts in the integrable case to compute, for a given initial condition q_0, the distance to the conjugate locus corresponding to short and long periodic trajectories.

C. Robustness issues

An important issue in quantum control is the robustness of the control with respect to boundary conditions and parameter uncertainties since the control is implemented as an open loop function. An example in given by the spin 1/2 case in NMR where the action of the magnetic field is related to the exact position of each particle. Clearly our analysis allows one to handle this problem. The Hamilton–Jacobi–Bellman approach permits one to analyze the sensitivity with respect to the boundary conditions, while the continuation method is a tool to determine the sensitivity of the control with respect to the dissipative parameters.

D. Numerical simulations

We next present the numerical results using the adapted numerical codes.

1. Application in nuclear magnetic resonance

We present in this section a numerical application in NMR. We consider the control of a spin 1/2 particle whose dynamics is governed by the Bloch equation,

$$\begin{pmatrix}\dot{M}_x\\ \dot{M}_y\\ \dot{M}_z\end{pmatrix}=\begin{pmatrix}-M_x/T_2\\ -M_y/T_2\\ (M_0-M_z)/T_1\end{pmatrix}+\begin{pmatrix}\omega_y M_z\\ -\omega_x M_z\\ \omega_x M_y-\omega_y M_x\end{pmatrix},$$

where $\vec{M}$ is the magnetization vector and $\vec{M}_0=M_0\vec{e}_z$ is the equilibrium point of the dynamics.[31] Since the initial point of the dynamics is on the z-axis, we assume that the dynamics is controlled through only one magnetic field along the x-axis. The typical value of the amplitude of the control field is denoted by $\omega_{\max}$. We introduce normalized coordinates $\vec{x}=(x,y,z)=\vec{M}/M_0$, a normalized control field $u_x=2\pi\omega_x/\omega_{\max}$ and a normalized time $\tau=\omega_{\max}t/(2\pi)$. Dividing the previous system by $\omega_{\max}M_0/(2\pi)$, we get that the evolution of the normalized coordinates is given by the following equations:

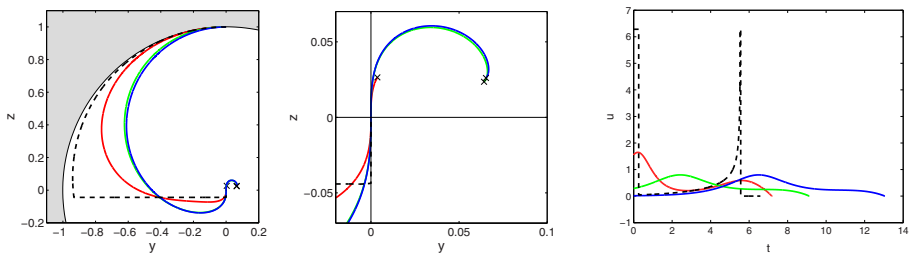

FIG. 7. (Color online) Plot of the different optimal trajectories (top) and of the corresponding control fields (bottom) for different control durations. Numerical values are, respectively, taken to be $K=1.1$, 1.5, and 2 for the red (dark gray), green (light gray), and blue (black) trajectories. The value $K=1$ refers to the time-minimum solution for the same dissipation parameters and a maximum normalized amplitude of the control field of 2π. The black crosses indicate the positions of the different conjugate points. The middle panel is a zoom of the top figure near the origin.

$$\begin{pmatrix} \dot{x} \\ \dot{y} \\ \dot{z} \end{pmatrix} = \begin{pmatrix} -\Gamma x \\ -\Gamma y \\ \gamma - \gamma z \end{pmatrix} + \begin{pmatrix} 0 \\ -u_x z \\ u_x y \end{pmatrix},$$

where $\Gamma=2\pi/(\omega_{\max}T_2)$ and $\gamma=2\pi/(\omega_{\max}T_1)$. Note that we have $\gamma=\gamma_+=\gamma_-$ in the previous notations of the dissipation parameters and that the equilibrium state of the dynamics is now the north pole of the Bloch sphere. Following Ref. 28, we consider the control problem of bringing the magnetization vector from the equilibrium point $\vec{M}_0$ to the center of the Bloch ball which corresponds to the zero-magnetization vector. Possible numerical values for the dissipation parameters are given by the experiments implemented in Ref. 28. The experiments were performed at room temperature with the proton spins of H_2O. The parameters were taken to be $T_1=740$ ms, $T_2=60$ ms, which correspond for $\omega_{\max}/(2\pi)=32.3$ Hz to $\gamma^{-1}=23.9$ and $\Gamma^{-1}=1.94$. We introduce $T_{\min}$ which is the minimum time to reach the target point with the constraint $|\omega|\leqslant\omega_{\max}$.[28] With the parameters T_1 and T_2, the time-optimal sequence has a duration of 202 ms.

Different numerical results about the structure of the extremal trajectories and the conjugate point analysis are displayed in Figs. 6 and 7. The description is based on a direct integration of the extremal equations. The optimal solutions have been obtained by solving the shooting equation with a Newton-type algorithm. No problem of convergence has been encountered in the different computations and the target state has been reached with a great accuracy.

In Fig. 6, we analyze the relation between the optimal trajectory and the dissipation parameters. We consider a control duration of $1.5\times T_{\min}$. The variation of $\delta=\Gamma-\gamma$ is realized by changing the value of Γ. In Fig. 7, we consider the dissipation parameters of Ref. 28 for the different trajectories but we modify the control duration which is given by $K\times T_{\min}$, where K is a scaling

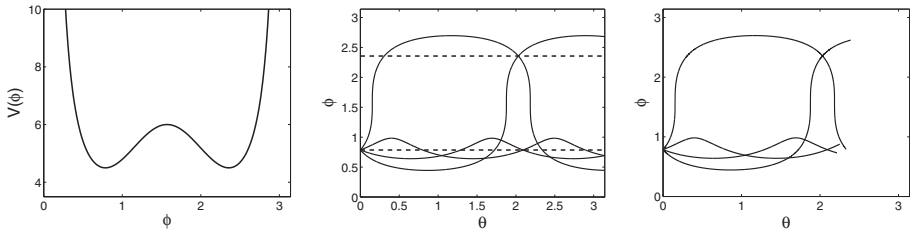

FIG. 8. (a) Plot of the potential V as a function of ϕ. (b) Plot of four extremals corresponding to $p_\phi(0)=-1$, 0, 1, and 2. (c) Same as (b) but up to the first conjugate point. Other numerical values are taken to be $\Gamma=3$, $\gamma_+=2$, $\phi=\pi/4$, $p_\rho=-2$, and $p_\theta=1$. The extremals associated with $p_\phi(0)=0$ and 1 are short periodic orbits with an energy equal to 5.5, while extremals with initial adjoint states $p_\phi(0)=-1$ and 2 are long periodic orbits with an energy equal to 6.5. The horizontal dashed lines indicate the positions of the parallel of equation $\phi=\pi/4$ and the antipodal one of equation $\phi=3\pi/4$ where short and long periodic orbits, respectively, intersect with the same time.

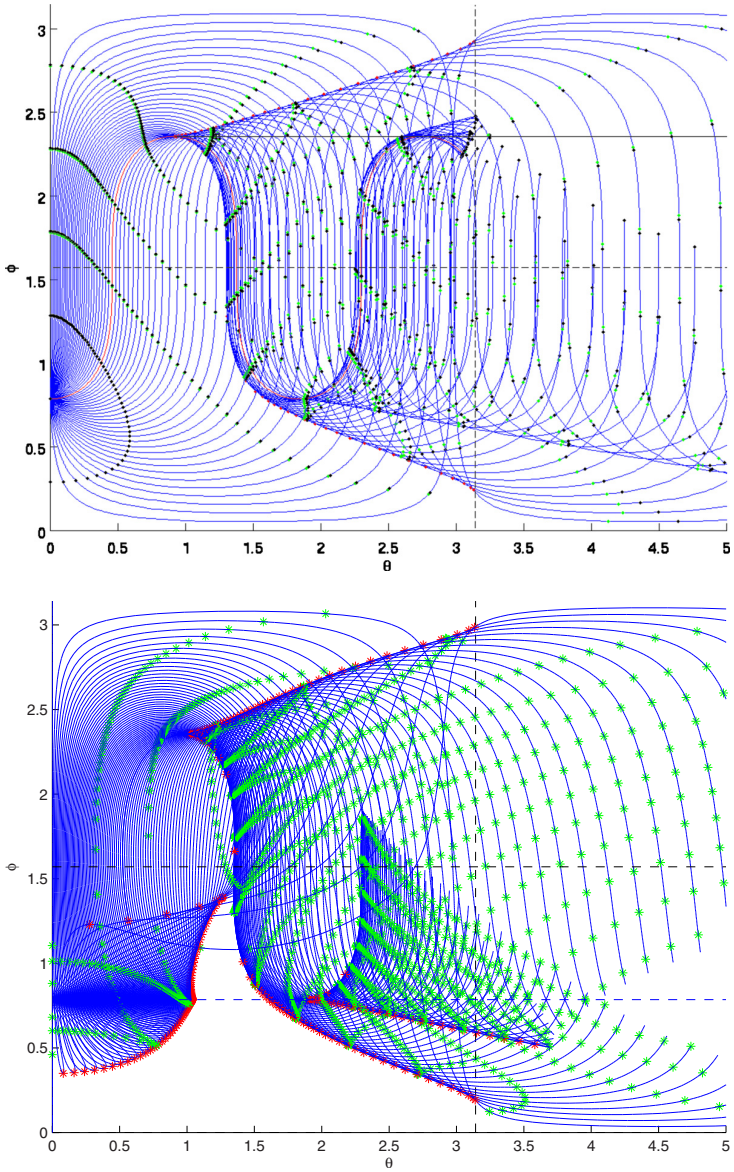

FIG. 9. (Color online) Conjugate loci, spheres, and wave fronts for the Grushin (top) and the non-Grushin case (bottom).

parameter. The results show that the structure of the extremals is simple. Note the similar behavior of the extremal trajectories when the dissipation parameters or the control duration are varied. We also indicate that all these trajectories could be implemented experimentally in NMR with the state of the art technology.[28] In Fig. 7, we have also evaluated the positions of the conjugate points. For different control durations, we observe in Fig. 7 that the first conjugate point appears after the target state. This means that the extremals are locally optimal up to the center of the Bloch ball. Other global properties of the extremals can be mentioned. We have checked that the total energy $\int_0^T u(t)^2 dt$ of the control field and the maximum of this control field decrease as T increases. This means that the maximum amplitude of $u(t)$ can be adjusted by choosing adequately the control duration. In Fig. 7, we compare the time-optimal solution computed in Ref. 28 with the solutions in the energy minimum case. The time-optimal solution is composed of two bang pulses of

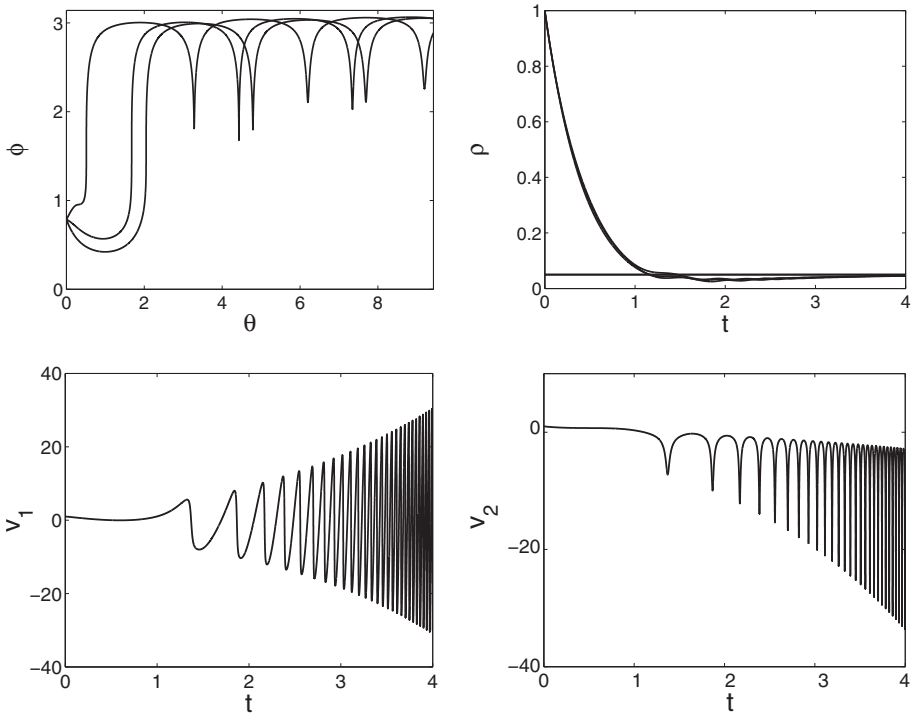

FIG. 10. (a) Evolution of the angle ϕ as a function of the angle θ for $\Gamma=2.5$, $\gamma_+=2$, and $\gamma_-=-0.1$. Initial values are taken to be $\phi(0)=\pi/4$, $p_\rho(0)=-10$, $p_\theta=1$, and $p_\phi(0)=-1$, 0, and 1. (b) Evolution of the radial coordinate ρ as a function of time. [(c) and (d)] Plot of the two optimal control fields v_1 and v_2 as a function of time for $p_\phi(0)=1$.

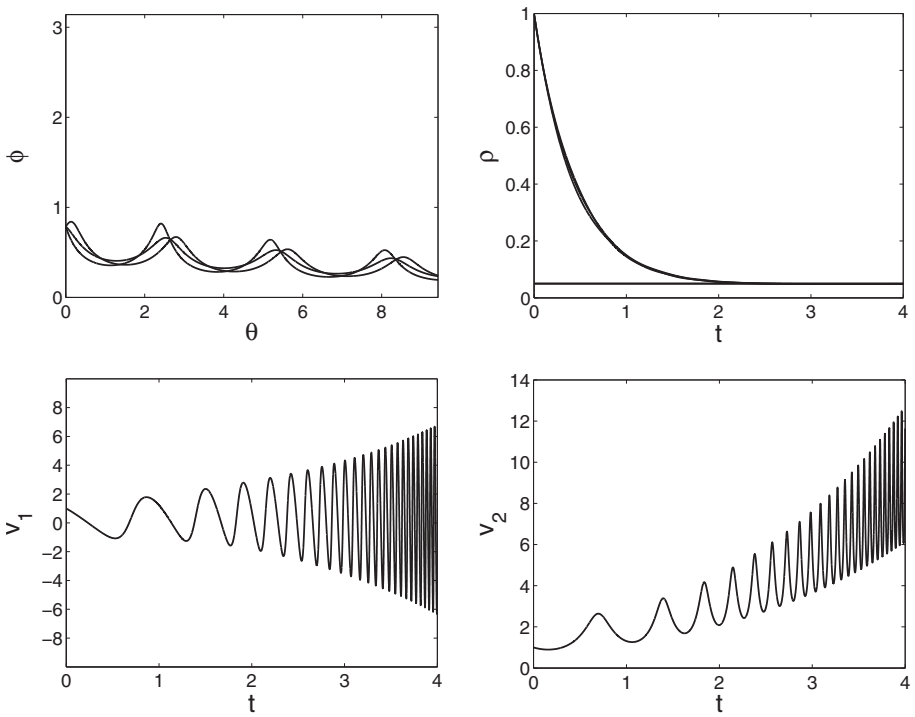

FIG. 11. The same as Fig. 10 but for $\gamma_-=0.1$.

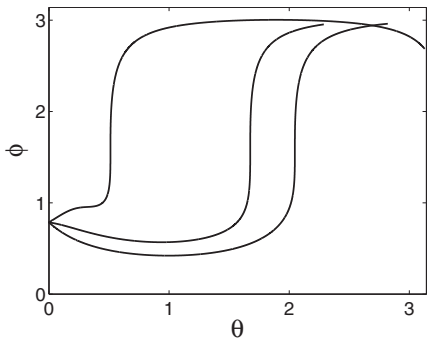

FIG. 12. The same as Fig. 10 but the extremals are plotted up to the first conjugate point.

maximum amplitude 2π and two singular controls. When the control duration is close to $T_{\min}$, i.e., when K is close to 1, we see that the structure of the optimal solution for the energy minimization case is close to the one for the time-optimal case.

2. Extremals and conjugate points in the integrable case

We illustrate in this section the different analytical results obtained in the integrable case. We consider the case of Fig. 8 where both short and long periodic orbits exist. In this example, we only modify the value of $p_\phi(0)$ to change the energy h of the system. We, respectively, obtain short and long orbits for $h<6$ and $h>6$. For p_ρ and p_θ fixed, there exist two trajectories starting from $(r(0),\phi(0),\theta(0))$ which intersect with the same cost on the antipodal parallel $(\phi=\pi-\phi(0))$ for long periodic orbits and on the initial parallel $(\phi=\phi(0))$ for short periodic orbits. These two extremals are defined by the two values of $p_\phi(0)$ for which the energy is the same. Such trajectories are displayed in Fig. 8 both for long and short periodic orbits. We have also determined by using the COTCOT code the position of the first conjugate points for these extremals.

3. Conjugate loci, spheres, and wave fronts

We represent in Fig. 9 the conjugate loci, the spheres, and the wave fronts for $T=5.5$, $\delta=1$, $\gamma_-=0$ and for the initial condition $\phi(0)=\pi/4$. We observe the existence of two microlocal situations corresponding to short and long periodic trajectories. For the second case, this corresponds to the persistence of a Grushin-type situation, represented in the same picture, for comparison.

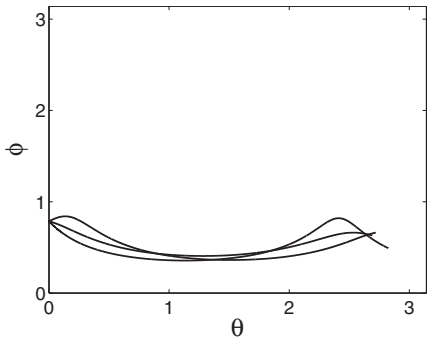

FIG. 13. The same as Fig. 12 but for $\gamma_-=-0.1$.

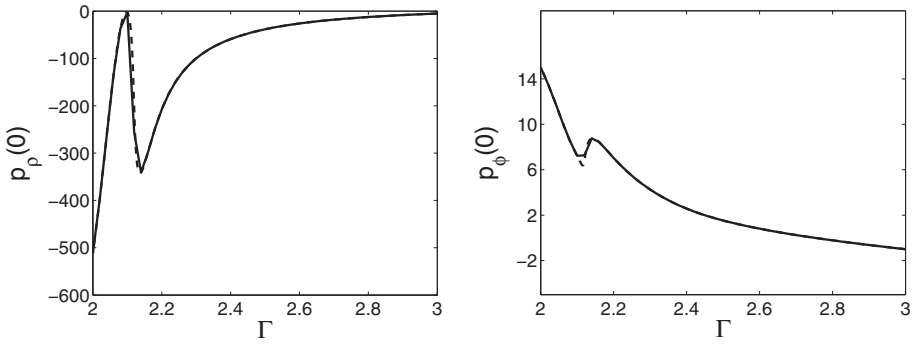

FIG. 14. Evolution as a function of the parameter Γ of the initial adjoint states $p_\rho(0)$, $p_\phi(0)$, and $p_\theta(0)$ for the Newton-type continuation (solid line) and the smooth-type one (dashed line). The other dissipative parameters are $\gamma_+=2$ and $\gamma_-=0.1$ and the control duration is equal to 0.5. The coordinates of the initial point are equal to $\phi(0)=\pi/4$, $\rho(0)=1$, $\theta(0)=0$, $p_\rho(0)=-5$, $p_\phi(0)=-1$, and $p_\theta(0)=1$ for $\Gamma=3$. The target state is ($\rho_f=0.3534$, $\phi_f=0.6004$, $\theta_f=2.0534$).

4. Extremals and conjugate points in the nonintegrable case

Using a direct integration of the Hamiltonian system we detail in this section the behavior of the extremals in the case $\gamma_- \neq 0$. The asymptotic behavior when $t \to +\infty$ is described for any values of Γ and γ_+ by the following conjecture based on numerical computations.

Conjecture 1: The asymptotic stationary points $(\rho_f, \phi_f, \theta_f)$ are characterized by $\rho_f = |\gamma_-| / \gamma_+$, and $\phi_f = 0$ if $\gamma_- > 0$ or $\phi_f = \pi$ if $\gamma_- < 0$.

Using the Hamiltonian equations, it is straightforward to show that $(\rho_f, \phi_f, \theta_f)$ satisfy

$$\gamma_- \cos \phi_f = \rho_f (\gamma_+ \cos^2 \phi_f + \Gamma \sin^2 \phi_f),$$

from which one deduces Conjecture 1. The different behaviors of the extremals are represented in Fig. 10 for $\gamma_- < 0$ and in Fig. 11 for $\gamma_- > 0$. After a complicated transient oscillatory structure, every extremal has the same asymptotic limit given by the conjecture 1. This also illustrates the robustness of the control with respect to parameter uncertainties since the asymptotic behavior of the extremals only depends on the sign of γ_- and not on γ_+ or Γ. This point could be important in view of possible experimental applications in NMR of these optimal control laws. Note also the unbounded and oscillatory behaviors of the two control fields v_1 and v_2. Finally, we have used the COTCOT code to evaluate the position of the conjugate points. As can be checked in Figs. 12 and 13, we observe that every extremal possesses a conjugate point, which was not the case in the time-minimal control of the same system.[11]

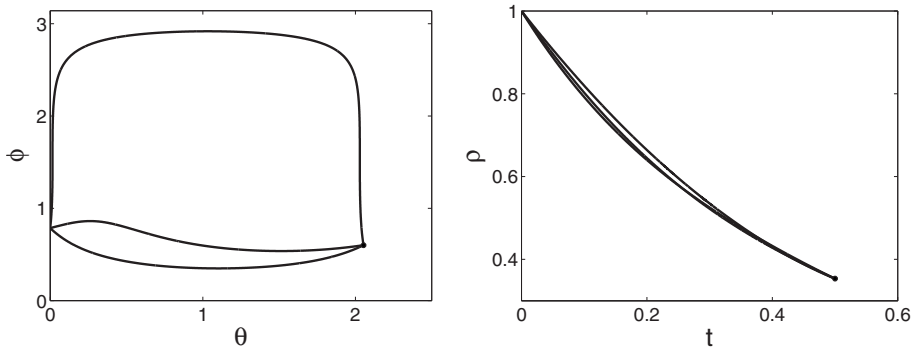

FIG. 15. Three extremal trajectories solutions of the smooth continuation method for $\Gamma=2$, 2.5, and 3. The black dot indicates the position of the target state.

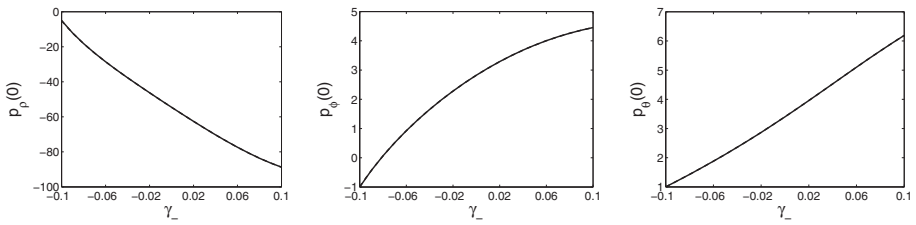

FIG. 16. The same as Fig. 14 but for a continuation in γ_-. The other dissipative parameters are $\Gamma=2.5$ and $\gamma_+=2$ and the control duration is equal to 0.5. The coordinates of the initial point are equal to $\phi(0)=\pi/4$, $\rho(0)=1$, $\theta(0)=0$, $p_\rho(0)=-5$, $p_\phi(0)=-1$, and $p_\theta(0)=1$ for $\gamma_-=-0.1$. The target state is ($\rho_f=0.314\,95$, $\phi_f=0.567\,126$, $\theta_f=1.242\,71$).

5. Continuation results

The smooth and the discrete continuation approaches have been implemented on two examples. We consider a continuation problem as a function of the parameter Γ in Figs. 14 and 15 and as a function of γ_- in Figs. 16 and 17. In the two cases, we fix a target state of coordinates $(\rho_f, \phi_f, \theta_f)$ and the control duration to $T=0.5$. The corresponding adjoint state $(p_\rho(0), p_\phi(0), p_\theta(0))$ solutions of this optimal control problem are known at the starting point of the continuation. We then use the two continuation algorithms to determine the new adjoint states such that the system reaches the same target state with the same control duration when the dissipative parameters vary. In the two cases, the control duration is chosen sufficiently small to be before the first conjugate point, which ensures the convergence of the continuation method.[13] Some accessibility problems can also be encountered for long times. Indeed, one has to check that the target state belongs to the accessible set of the initial point when the dissipative parameters vary. Due to the dissipation effects, this is done numerically for each value of the continuation parameter . The step sizes of the discrete approach are, respectively, equal to 0.02 and 0.01 for the continuations in Γ and γ_-, while is not fixed for the smooth one. With this step size, the Newton algorithm does not encounter any problem to converge. The shooting equation is solved at each step with an accuracy of the order of 10^{-12}. We have also observed that this size has to be increased when the control duration increases. Note the different behaviors of the two approaches in Fig. 17, which displays the evolution of the continuation parameter as a function of the number of steps. In the two examples, we remark that the number of steps needed by the smooth approach is larger than in the discrete case (Fig. 18). A larger step size can be used in the discrete method because the shooting equation is solved at each step, which is not the case for the smooth method. The different initial adjoint states represented in Figs. 14 and 15 show that the results obtained by the two methods are similar. Note the large variations of the adjoint states, which are due to the relatively large modifications

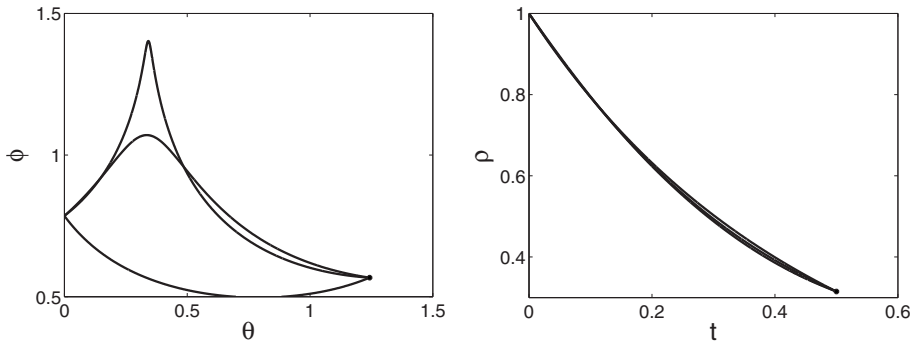

FIG. 17. Three extremal trajectories solutions of the smooth continuation method for $\gamma_-=-0.1$, 0, and 0.1. The black dot indicates the position of the target state.

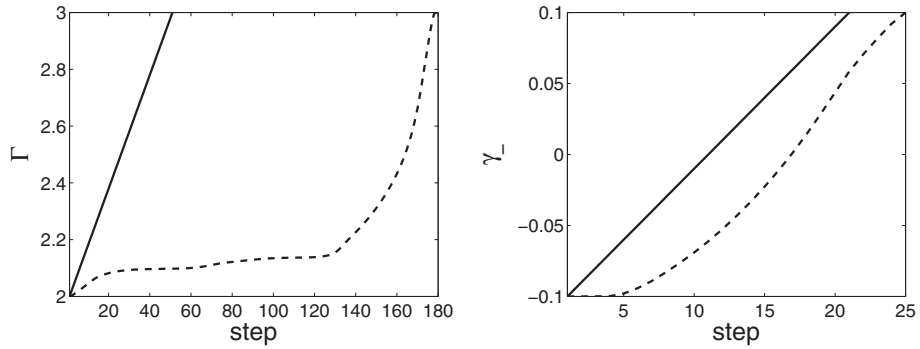

FIG. 18. Evolution of the continuation parameters as a function of the number of steps for the discrete method (solid line) and the smooth one (dashed line).

of the shape of the optimal trajectories when the dissipative parameters, vary (see Figs. 15 and 17). This indicates the very good behavior of the continuation approach in this problem.

[1] Abramowitz, M. and Stegun, I. A., *Handbook of Mathematical Functions* (Dover, New York).
[2] Agrachev, A. A., Chtcherbakova, N. N., and Zelenko, I., "On curvatures and focal points of dynamical lagrangian distributions and their reductions by first integrals," J. Dyn. Control Syst. **11**, 297 (2005).
[3] Aguilar, J.-P. and Berglund, N., "The effect of classical noise on a quantum two-level system," J. Math. Phys. **49**, 102102 (2008).
[4] D'Alessandro, D., *Introduction to Quantum Control and Dynamics*, CRC Applied Mathematics and Nonlinear Science Series (Chapman and Hall, Boca Raton, 2008).
[5] D'Alessandro, D. and Dahled, M., "Optimal control of two-level quantum systems," IEEE Trans. Autom. Control **46**, 866 (2001).
[6] Allgower, E. L. and Georg, K., *Introduction to Numerical Continuation Methods*, Classics in Applied Mathematics Vol. 45 (SIAM), Philadelphia, PA, 2003. (reprint of the 1990 edition [Springer-Verlag, Berlin; MR1059455 (92a:65165)]).
[7] Audin, M., *Les Systèmes Hamiltoniens et leur intégrabilité (French) [Hamiltonian Systems and Their Integrability]*, Cours Spécialisés [Specialized Courses] Vol. 8 (Société Mathématique de France, Paris EDP Sciences, Les Ulis, 2001), pp. 1–170 (French).
[8] Bonnard, B., Caillau, J.-B., Sinclair, R., and Tanaka, M., "Conjugate and cut loci of a two-sphere of revolution with application to optimal control," Ann. Inst. Henri Poincaré, Anal. Non Linéaire **26**, 1081 (2009).
[9] Bonnard, B., Caillau, J.-B., and Trélat, E., "Second order optimality conditions in the smooth case and applications in optimal control," ESAIM: COCV **13**, 207 (2007).
[10] Bonnard, B. and Chyba, M., *Singular Trajectories and Their Role in Control Theory*, Mathematiques and Applications [Mathematics and Applications] Vol. 40 (Springer-Verlag, Berlin, 2003) (Berlin).
[11] Bonnard, B., Chyba, M., and Sugny, D., "Time-minimal control of dissipative two-level quantum systems: The generic case," IEEE Trans. Autom. Control **54**, 2598 (2009).
[12] Bonnard, B. and Kupka, I., "Théorie des singularités de l'application entrée-sortie et optimalité des trajectoires singulières dans le problème du temps minimal," Forum Math. **5**, 111 (1993).
[13] Bonnard, B., Shcherbakova, N., and Sugny, D., "The smooth continuation method in optimal control with an application to quantum systems," ESAIM: COCV.
[14] Bonnard, B. and Sugny, D., "Time-minimal control of dissipative two-level quantum systems: The integrable case," SIAM J. Control Optim. **48**, 1289 (2009).
[15] Bonnard, B. and Sugny, D., "Geometric optimal control and two-level dissipative quantum systems," Contr. Cybernet. **38**, 1053 (2009).
[16] Boscain, U., Charlot, G., Gauthier, J.-P., Guérin, S., and Jauslin, H.-R., "Optimal control in laser-induced population transfer for two- and three-level quantum systems," J. Math. Phys. **43**, 2107 (2002).
[17] Boscain, U. and Mason, P., "Time minimal trajectories for a spin 1/2 particle in a magnetic field," J. Math. Phys. **47**, 062101 (2006).
[18] Bruce, J. W. and Giblin, P. J., *Curves and Singularities: A Geometrical Introduction to Singularity Theory*, 2nd ed. (Cambridge University Press, Cambridge, 1992), pp. 1–321.
[19] COTCOT: http://apo.enseeiht.fr/cotcot/.
[20] Davies, H., *Introduction to Non Linear and Integral Equations* (Dover, New York, 1990).
[21] do Carmo, M. P., *Riemannian Geometry* (Birkhäuser, Boston, 1992).
[22] Gorini, V., Kossakowski, A., and Sudarshan, E. C. G., "Completely positive dynamical semigroups of *N*-level systems," J. Math. Phys. **17**, 821 (1976).
[23] Goryunov, V. V. and Zakalyukin, V. M., "Lagrangian and Legendrian singularities," *Singularity theory* (World Scientific, Hackensack, NJ, 2007), pp. 157–186.
[24] Guerra, M. and Sarychev, A., "Existence and Lipschitzian regularity for relaxed minimizers," *Mathematical Control*

Theory and Finance (Springer, New York, 2008), pp. 231–250.
[25] Khaneja, N., Brockett, R., and Glaser, S. J., "Time optimal control in spin systems," Phys. Rev. A **63**, 032308 (2001).
[26] Khaneja, N., Glaser, S. J., and Brockett, R., "Sub-Riemannian geometry and time optimal control of three spin systems: Quantum gates and coherence transfer," Phys. Rev. A **65**, 032301 (2002).
[27] Kupka, I. (private communication).
[28] Lapert, M., Zhang, Y., Braun, M., Glaser, S. J., and Sugny, D., "Singular extremals for the time-optimal control of dissipative spin 1/2 particles," Phys. Rev. Lett. **104**, 083001 (2010); Assémat, E., Lapert, M., Zhang, Y., Braun, M., Glaser, S. J., and Sugny, D., "Simultaneous time-optimal control of the inversion of two spin-1/2 particles," Phys. Rev. A **82**, 013415 (2010).
[29] Lawden, D. F., *Elliptic Functions and Applications*, Applied Mathematical Sciences Vol. 80 (Springer-Verlag, New York, 1989), pp. 1–334.
[30] Lee, E. B. and Markus, L., *Foundations of Optimal Control Theory* (Wiley, New York, 1967), pp. 1–576.
[31] Levitt, M. H., *Spin Dynamics: Basics of Nuclear Magnetic Resonance* (Wiley, New York, 2008).
[32] Lindblad, G., "On the generators of quantum dynamical semigroups," Commun. Math. Phys. **48**, 119 (1976).
[33] Meyer, K. R. and Hall, G. R., *Introduction to Hamiltonian Dynamical Systems and the N-Body Problem*, Applied Mathematical Sciences Vol. 90 (Springer-Verlag, New York, 1992), pp. 1–292.
[34] Mirrahimi, M. and Rouchon, P., "Singular perturbations and Lindblad-Kossakowski differential equations," IEEE Trans. Autom. Control **54**, 1325 (2009).
[35] Nemytskii, V. V. and Stepanov, V. V., *Qualitative Theory of Differential Equations*, Princeton Mathematical Series, No. 22 (Princeton University Press, Princeton, NJ, 1960), pp. 1–523.
[36] Pontryagin, L. S., Boltyanskii, V. G., Gamkrelidze, R. V., and Mishchenko, E. F., in *The Mathematical Theory of Optimal Processes*, translated from the Russian by K. N. Trirogoff, edited by L. W. Neustadt (Wiley, New York, 1962), pp. 1–360.
[37] Ramakrishna, S. and Seideman, T., "Intense laser alignment in dissipative media as a route to solvent dynamics," Phys. Rev. Lett. **95**, 113001 (2005).
[38] Stefanatos, D., "Optimal design of minimum-energy pulses for Bloch equations in the case of dominant transverse relaxation," Phys. Rev. A **80**, 045401 (2009).
[39] Sugny, D., Kontz, C., and Jauslin, H. R., "Time-optimal control of a two-level dissipative quantum system," Phys. Rev. A **76**, 023419 (2007).
[40] Trélat, E., "Etude asymptotique et transcendance de la fonction valeur en contrôle optimal; catégorie log-exp en géométrie sous-Riemannienne dans le cas Martinet," Ph.D. thesis, University of Burgundy, (2000).
[41] Trélat, E., "Some properties of the value function and its level sets for affine control systems with quadratic cost," J. Dyn. Control Syst. **6**, 511 (2000).
[42] Vieillard, T., Chaussard, F., Sugny, D., Lavorel, B., and Faucher, O., "Field-free molecular alignment of CO_2 mixtures in presence of collisional relaxation," J. Raman Spectrosc. **39**, 694 (2008).